[AMERICAN JOURNAL OF SCIENCE, VOL. 283, SEPTEMBER, 1983, P. 641-683]

American Journal of Science

*SEPTEMBER 1983*

# THE CARBONATE-SILICATE GEOCHEMICAL CYCLE AND ITS EFFECT ON ATMOSPHERIC CARBON DIOXIDE OVER THE PAST 100 MILLION YEARS

ROBERT A. BERNER,* ANTONIO C. LASAGA,** and ROBERT M. GARRELS***

**ABSTRACT.** A computer model has been constructed that considers the effects on the $CO_2$ level of the atmosphere, and the Ca, Mg, and $HCO_3$ levels of the ocean, of the following processes: weathering on the continents of calcite, dolomite, and calcium-and-magnesium-containing silicates; biogenic precipitation and removal of $CaCO_3$ from the ocean; removal of Mg from the ocean via volcanic-seawater reaction; and the metamorphic-magmatic decarbonation of calcite and dolomite (and resulting $CO_2$ degassing) as a consequence of plate subduction. Assuming steady state, values for fluxes to and from the atmosphere and oceans are first derived for the modern ocean-atmosphere system. Then the consequences of perturbing steady state are examined by deriving rate expressions for all transfer reactions. These rate expressions are constructed so as to reflect changes over the past 100 my in the following rate-controlling parameters: continental land area as it affects total weathering fluxes; seafloor spreading rate as it affects metamorphic-magmatic decarbonation and uptake of oceanic Mg by basalt-seawater reaction; the monotonic conversion of dolomite to calcite plus Mg-silicates as it affects both weathering and metamorphic decarbonation rates; the $CO_2$ level of the atmosphere as it affects worldwide air temperature and, consequently, both weathering rate and continental runoff; and the Ca and $HCO_3$ of the ocean along with the $CO_2$ content of the atmosphere as they together affect the rate of $CaCO_3$ removal from the oceans. In the latter two cases functional dependencies on $CO_2$, Ca, and $HCO_3$ are set up so as to provide negative feedback to the system. An initial condition is constructed for 100 my BP, and a set of eight differential mass balance equations are then solved simultaneously as the system is allowed to evolve toward the present, with care being taken in choosing the initial condition so as to insure that actual present-day values are recovered at the end of each run.

* Department of Geology and Geophysics, Yale University, New Haven, Connecticut 06511

** Department of Geosciences, Pennsylvania State University, University Park, Pennsylvania 16802

*** Department of Marine Science, University of South Florida, 140 7th Avenue-South, St. Petersburg, Florida 33701

**Results indicate that the $CO_2$ content of the atmosphere is highly sensitive to changes in seafloor spreading rate and continental land area, and, to a much lesser extent, to changes in the relative masses of calcite and dolomite. Consideration of a number of alternative seafloor spreading rate formulations shows that in all cases a several-fold higher $CO_2$ level for the Cretaceous atmosphere (65-100 my BP) is obtained via the model. Assuming that $CO_2$ level and surface air temperature are positively correlated via an atmospheric greenhouse model, we predict Cretaceous paleotemperatures which are in rough general agreement with independent published data. Consequently, our results point to plate tectonics, as it affects both metamorphic-magmatic decarbonation and changes in continental land area, as a major control of world climate.**

## INTRODUCTION

Since the classic work of Urey (1952) it has been often postulated that, over geologic time scales, the level of atmospheric carbon dioxide is greatly affected, if not controlled by, the transformation of silicate rocks to carbonate rocks by weathering and sedimentation and retransformation back to silicate rocks by metamorphism and magmatism (see also Holland, 1978; Budyko and Ronov, 1979; Mackenzie and Pigott, 1981; and Fischer, 1983). The classic "Urey reactions" can be written as:

$$CO_2 + CaSiO_3 \underset{\text{metamorphism}}{\overset{\text{weathering}}{\rightleftharpoons}} CaCO_3 + SiO_2$$

$$CO_2 + MgSiO_3 \underset{\text{metamorphism}}{\overset{\text{weathering}}{\rightleftharpoons}} MgCO_3 + SiO_2$$

(Here $CaSiO_3$ and $MgSiO_3$ can be interpreted as representing any high temperature calcium and magnesium silicate, not simply wollastonite and enstatite; $SiO_2$ as representing sedimentary silicates; and $MgCO_3$ as the $MgCO_3$ component of dolomite.) The level of atmospheric $CO_2$ results from a balance between uptake by weathering and release by metamorphism-magmatism, and this constitutes the usual carbonate-silicate geochemical cycle. Perturbations of forward and backward reactions can result in an imbalance in rates which may, in turn, bring about changes in the level of atmospheric $CO_2$.

Carbon dioxide is involved also in the weathering of carbonate minerals (calcite and dolomite) as well as in their precipitation in the oceans. Another classic reversible reaction, alluded to by Chamberlin (1898), is:

$$CO_2 + CaCO_3 + H_2O \underset{\text{precipitation}}{\overset{\text{weathering}}{\rightleftharpoons}} Ca^{++} + 2HCO_3^-$$

A similar reaction for dolomite is:

$$2CO_2 + CaMg(CO_3)_2 + 2H_2O \underset{\text{precipitation}}{\overset{\text{weathering}}{\rightleftharpoons}} Ca^{++} + Mg^{++} + 4HCO_3^-$$

Perturbation of these weathering-precipitation reactions (perturbation of the former pointed out by Chamberlin, 1898) can also result in imbalances and changes in both the chemistry of seawater and the level of atmospheric $CO_2$. In this way, carbonate weathering and precipitation can be added to silicate weathering and metamorphism-magmatism as major processes in the carbonate-silicate geochemical cycle.

Several major changes have occurred at the Earth's surface over the past 100 my which must have exerted some effect on the level of atmospheric $CO_2$ (Fischer, 1983). Two of these changes are tectonic in origin. If changes in spreading rates of lithospheric plates over this time can be used as a guide to changes in worldwide tectonism, there should have been corresponding changes in rates of $CO_2$ addition to the atmosphere via tectonically-induced metamorphism and magmatism. This is true both of descending plate boundaries, where much $CO_2$ release due to heating and decarbonation occurs (for example, Barnes, Irwin, and White, 1978), and mid-oceanic rises where carbonate-derived $CO_2$ circulated through the mantle is degassed to the ocean-plus-atmosphere (Javoy, Pineau, and Allegre, 1982). In either case increased plate motion should be accompanied by increased $CO_2$ outgassing. The other effect of tectonics is to bring about changes in the area of the continents due to changes in sea-level accompanying changes in spreading rates (for example, Hays and Pitman, 1973; Pitman, 1978). Changes in continental area should affect directly the rate of $CO_2$ removal from the atmosphere by altering the amount of land available for rock weathering.

Besides tectonic factors over the past 200 my there has been a much lower rate of formation of sedimentary dolomite, $CaMg(CO_3)_2$, from seawater as compared to previous times. This was pointed out as early as 1909 by Daly and is evidenced by a virtual absence of this mineral from late Mesozoic and Cenozoic rocks (for example, see Garrels and Mackenzie, 1971, for a recent discussion). As a result, Mg removal from the oceans over this period has occurred primarily as silicate minerals (via volcanic-seawater reaction), while Ca removal has taken place almost entirely as $CaCO_3$. The net result (Holland, 1978) is that there has been a transfer of magnesium from the carbonate to the silicate reservoir in exchange for calcium:

$$CaMg(CO_3)_2 + CaSiO_3 \rightarrow 2CaCO_3 + MgSiO_3$$

Because of these changes in the masses of dolomite and calcite, it is possible that an additional perturbation has occurred in the carbonate-silicate cycle which has affected the level of atmospheric carbon dioxide.

In the present paper we will examine the hypothesis that atmospheric $CO_2$ has changed in the geologic past by constructing the carbonate-silicate cycle for the present and seeing how it has changed over the past 100 my. In this way we can test for the relative importance of tectonism and changes in the mass of sedimentary dolomite as major factors affecting $CO_2$. Throughout our discussion we will ignore the effects of the photosynthetic-respiration, or organic, cycle on $CO_2$. This is justifiable for live organisms because of the smallness of the biosphere carbon reservoir and the extreme rapidity of its turnover (for example, see Plass, 1956; or Holland, 1978). However, for sedimentary organic matter the masses of carbon are not negligible, and the turnover of this carbon via oxidation during weathering and reduction during sedimentation can affect atmospheric $CO_2$ levels on a geologic time scale (for example, see Garrels, Lerman, and Mackenzie, 1976). We will assume, nevertheless, that for the past 100 my this long-term organic cycle is perfectly in balance. This is obviously an oversimplification, but it enables us to examine the effects of the carbonate-silicate cycle on atmospheric $CO_2$ without additional complications. Besides, it is not too unreasonable. Examination of trends in the carbon and sulfur isotopic composition of the oceans over this period indicates that changes in the rate of sedimentary organic carbon burial (Garrels and Lerman, 1981) have been distinctly less than changes in the rate of $CO_2$ uptake by weathering or $CO_2$ degassing by metamorphic-volcanic activity.

Another assumption that we will make, implicitly, is that $CO_2$ uptake during the weathering of sodium and potassium silicate minerals (15-20 percent of the total weathering $CO_2$ uptake — see Holland, 1978) is balanced by an equivalent $CO_2$-liberating process, and as a result the Na–K–$CO_2$ subcycle can be ignored. As will be seen later, this assumption is reasonably good and should not appreciably affect our results.

## PRESENT-DAY CARBONATE-SILICATE CYCLE

Before discussing changes in the carbonate-silicate cycle over the past 100 my and its effect on atmospheric $CO_2$, it is necessary to construct a present day cycle to demonstrate the relative magnitudes of the various processes involved in it. Much of our discussion parallels that of Holland (1978) with the major differences being that new weathering data are employed, weathering by sulfuric acid is considered, and a greater role is assigned to volcanic-seawater reaction.

*Weathering fluxes.*—The present-day rates of weathering of dolomite, calcite (used here loosely to represent both calcite and aragonite), calcium silicates, and magnesium silicates are derived by determining the relative contributions of each to the composition of world average river water and by multiplying these values by the flow of river water to the sea. For the purposes of calculation, we will use the values taken from Meybeck (1979), for natural (corrected for pollution) average river water composition and flow. They are:

$$[Ca^{++}] = 13.4 \text{ mg per liter} \qquad (1)$$

$$[Mg^{++}] = 3.35 \text{ mg per liter} \quad (2)$$

$$Q = 3.74 \times 10^{16} \text{ liters per yr} \quad (3)$$

Here the brackets represent concentrations, and Q is the total annual flow of river water to the oceans. Converting to moles and multiplying Q by the concentrations, we obtain the total fluxes, $F^*_{Ca_T}$ and $F_{Mg_T}$.

$$F^*_{Ca_T} = 12.5 \times 10^{12} \text{ moles per yr} \quad (4)$$

$$F_{Mg_T} = 5.2 \times 10^{12} \text{ moles per yr} \quad (5)$$

(The asterisk denotes that the Ca flux is to undergo certain corrections.) These fluxes represent only continental additions due to weathering, because neither $Ca^{++}$ nor $Mg^{++}$ is appreciably affected by atmospheric cycling, and corrections for pollution have already been made.

Before dividing the calcium weathering flux into its component carbonate and silicate fluxes, we must make two corrections. First, there is a small correction for $Ca^{++}$ contributed by the weathering of $CaSO_4$ minerals (gypsum and anhydrite). This is done by assuming that the preman, pre-pollution natural river sulfate flux ($2.5 \times 10^{12}$ moles per yr) is made up of contributions from the weathering of pyrite and $CaSO_4$, from volcanism, and from atmospherically cycled sulfur. Contributions from the latter two sources are estimated to be approx $0.8 \times 10^{12}$ moles $SO_4$ per yr (Berner and Berner, 1984), whereas the flux from pyrite weathering is estimated as $0.5 \times 10^{12}$ moles per yr (Berner and Raiswell, 1983). Subtracting pyrite weathering, volcanic, and atmospheric-cyclic additions from the total, we obtain $1.2 \times 10^{12}$ moles per yr as the value of the $CaSO_4$ weathering flux. This is a reasonable value in comparison with the pyrite weathering flux and what is known about the relative abundances and reactivities of the two minerals (Berner, 1971; Berner and Berner, 1984).

The other correction to the $Ca^*_T$ flux takes into account the amount of riverine $Ca^{++}$ delivered to the oceans on solid particles which undergoes ion exchange upon entering the sea and consequent release to solution (for example, see Sayles and Mangelsdorf, 1977). From a consideration of the concentration of suspended matter in rivers, its ion exchange capacity and Ca content, and the degree of exchange in seawater, a value of 10 to 20 percent of the dissolved Ca flux has been derived by Holland (1978) for the particle-borne Ca-flux. This is equivalent to $1.9 \pm 0.7 \times 10^{12}$ moles yer yr.

Subtracting the $CaSO_4$-derived Ca flux ($1.2 \times 10^{12}$ moles per yr) and adding the particle-borne flux ($1.9 \times 10^{12}$ moles per yr), we obtain, finally, a corrected flux of Ca from carbonate and silicate weathering of:

$$F_{Ca_T} = 13.2 \times 10^{12} \text{ moles per yr} \quad (6)$$

Apportionment of the corrected Ca river flux to various carbonates and silicates is based on the following assumptions:

1. 75 percent of the continental area is underlain by sedimentary rocks with 25 percent underlain by igneous and metamorphic rocks (Holland, 1978).

2. The concentration of total dissolved solids (TDS) in waters draining sedimentary rocks is twice that of those draining igneous and metamorphic rocks (Holland, 1978).
3. The ratio Ca/TDS of waters draining sedimentary rocks is equal to that of waters draining igneous and metamorphic rocks.
4. 85 percent of Ca in sedimentary rocks is present as carbonates (calcite and dolomite) (Holland, 1978), and 15 percent as calcium silicates.
5. Ca in sedimentary carbonates weathers twice as fast as Ca in sedimentary silicates.

From assumptions 1, 2, and 3:

$$\frac{F_{Ca_{sed}}}{F_{Ca_{all\ rocks}}} = 0.86 \qquad \frac{F_{Ca_{ig\ +\ met}}}{F_{Ca_{all\ rocks}}} = 0.14 \tag{7}$$

where F = weathering flux carried by rivers to the oceans.
From assumptions 4 and 5:

$$F_{Ca_{sed\ carb}} = 11.3\ F_{Ca_{sed\ silc}} \tag{8}$$

where sed carb and sed silc refer to sedimentary carbonates and silicates respectively. Since:

$$F_{Ca_{sed}} = F_{Ca_{sed\ carb}} + F_{Ca_{sed\ silc}} \tag{9}$$

from eqs (7), (8), and (9):

$$\frac{F_{Ca_{sed\ carb}}}{F_{Ca_{all\ rocks}}} = 0.79 \tag{10}$$

$$\frac{F_{Ca_{sed\ silc}}}{F_{Ca_{all\ rocks}}} = 0.07 \tag{11}$$

$$\frac{F_{Ca_{ig+met}}}{F_{Ca_{all\ rocks}}} = 0.14 \tag{12}$$

also, from (6):

$$F_{Ca_{all\ rocks}} = F_{Ca_T} = 13.2 \times 10^{12}\ \text{moles per yr} \tag{13}$$

Apportionment of the total Mg river flux to various carbonates and silicates is based on the following expressions:

$$\frac{F_{Mg_{sed\ carb}}}{F_{Mg_{all\ rocks}}} = \left(\frac{F_{Mg_{sed\ carb}}}{F_{Ca_{sed\ carb}}}\right)\left(\frac{F_{Ca_{sed\ carb}}}{F_{Ca_{all\ rocks}}}\right)\left(\frac{F_{Ca_T}}{F_{Mg_T}}\right) \tag{14}$$

$$\frac{F_{Mg_{ig+met}}}{F_{Mg_{all\ rocks}}} = \left(\frac{F_{Mg_{ig+met}}}{F_{Ca_{ig+met}}}\right)\left(\frac{F_{Ca_{ig+met}}}{F_{Ca_{all\ rocks}}}\right)\left(\frac{F_{Ca_T}}{F_{Mg_T}}\right) \tag{15}$$

$$F_{Mg_{all\ rocks}} = F_{Mg_{sed\ carb}} + F_{Mg_{ig+met}} + F_{Mg_{sed\ silc}}. \tag{16}$$

In eq (14) we have used an Mg/Ca ratio for waters draining carbonate rocks of 0.2 based on the rock abundance data for figure 1 of the present

paper (see also Holland, 1978) and the assumption that calcite weathers slightly faster than dolomite. In eq (15) we use the value of average Mg/Ca for igneous and metamorphic rocks of 0.5 based on a mixture of 70 percent basalt (Mg/Ca = 0.7) and 30 percent granite (Mg/Ca = 0.2). From these values and those given in eqs (5), (6), (10), and (12) we obtain:

$$\frac{F_{Mg_{\text{sed carb}}}}{F_{Mg_{\text{all rocks}}}} = 0.40 \tag{17}$$

$$\frac{F_{Mg_{\text{sed silc}}}}{F_{Mg_{\text{all rocks}}}} = 0.42 \tag{18}$$

$$\frac{F_{Mg_{\text{ig and met}}}}{F_{Mg_{\text{all rocks}}}} = 0.18 \tag{19}$$

Also, from (5):

$$F_{Mg_{\text{all rocks}}} = F_{Mg_T} = 5.2 \times 10^{12} \text{ moles per yr} \tag{20}$$

Finally, we note that since dolomite is the source of almost all carbonate magnesium:

$$F_{Mg_{\text{sed carb}}} = F_{Mg_{\text{dol}}} \tag{21}$$

$$F_{Mg_{\text{dol}}} = F_{Ca_{\text{dol}}} \tag{22}$$

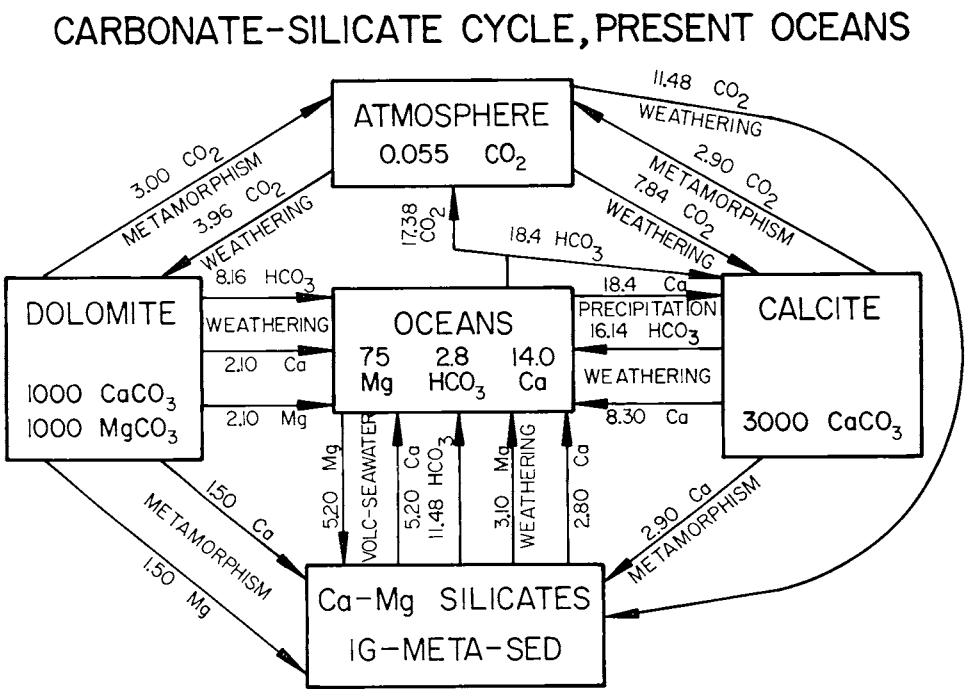


Fig. 1. Carbonate-silicate cycle for the present day. Fluxes of $CO_2$ and $HCO_3^-$ are corrected for weathering via $H_2SO_4$ (from pyrite oxidation) and for sedimentary pyrite formation (see text). Fluxes in $10^{18}$ moles per my; reservoir sizes in $10^{18}$ moles.

where the subscript dol refers to dolomite. On the basis of eqs (10) to (13) and (17) to (22), we have constructed table 1. Note that, for relevance to long term balances, units are given in $10^{18}$ moles per million years (my).

The fluxes of Ca and Mg listed in table 1 result from the attack of carbonic and sulfuric acids on carbonate and silicate minerals. Carbonic acid arises from $CO_2$ generated in soils by the microbial oxidation of organic matter, whereas sulfuric acid results from the oxidation during weathering of sulfides, mainly pyrite ($FeS_2$). Representative reactions are for acid generation:

$$CH_2O_{org} + O_2 \rightarrow CO_2 + H_2O$$

$$CO_2 + H_2O \rightarrow H_2CO_3$$

$$4FeS_2 + 15O_2 + 8H_2O \rightarrow 2Fe_2O_3 + 8H_2SO_4$$

and for mineral dissolution:

$$H_2CO_3 + CaCO_3 \rightarrow Ca^{++} + 2HCO_3^-$$

$$2H_2CO_3 + CaMg(CO_3)_2 \rightarrow Ca^{++} + Mg^{++} + 4HCO_3^-$$

$$2H_2CO_3 + MgSiO_3 + H_2O \rightarrow Mg^{++} + 2HCO_3^- + H_4SiO_4$$

$$H_2SO_4 + 2CaCO_3 \rightarrow 2Ca^{++} + 2HCO_3^- + SO_4^{--}$$

$$H_2SO_4 + CaMg(CO_3)_2 \rightarrow Ca^{++} + Mg^{++} + 2HCO_3^- + SO_4^{--}$$

$$H_2SO_4 + MgSiO_3 + H_2O \rightarrow Mg^{++} + SO_4^{--} + H_4SiO_4$$

The relative amounts of weathering by carbonic and sulfuric acids can be estimated as follows. Berner and Raiswell (1983) have estimated the preman rate of pyrite oxidation to $H_2SO_4$ to be $0.51 \times 10^{18}$ moles per my. If this $H_2SO_4$ is reacted with dolomite, calcite, and silicates in the same proportions as the total cation (Ca + Mg) fluxes from each mineral, it is divided into $0.12 \times 10^{18}$ moles $my^{-1}$ for dolomite weathering, $0.23 \times 10^{18}$ moles $my^{-1}$ for $CaCO_3$ weathering, and $0.16 \times 10^{18}$ moles $my^{-1}$ for silicate weathering. (Weathering of sodium and potassium silicate by sulfuric acid can be assumed to be negligible for present purposes.) Weathering by carbonic acid is then calculated by charge balance. Accompanying each

TABLE 1

River fluxes, F, of Ca and Mg resulting from the weathering of specific minerals or groups of minerals. Fluxes are in $10^{18}$ moles per my (= $10^{12}$ moles per yr)

| Mineral | $F_{Ca}$ | % | $F_{Mg}$ | % |
|---|---|---|---|---|
| calcite | 8.3 | 63 | — | — |
| dolomite | 2.1 | 16 | 2.1 | 40 |
| sed. Ca-silicates | 0.9 | 7 | — | — |
| ig. + met. Ca-silicates | 1.9 | 14 | — | — |
| sed. Mg-silicates | — | — | 2.2 | 42 |
| ig. + met. Mg-silicates | — | — | 0.9 | 18 |
| Total | 13.2 | 100 | 5.2 | 100 |

mole of $Ca^{++}$ plus $Mg^{++}$ must be an equivalent charge carried by $SO_4^{--}$ and $HCO_3^-$ (see the above weathering reactions). Subtracting the charge carried by the above values for $SO_4^{--}$ fluxes from the total required anion fluxes gives the charge carried by $HCO_3^-$. For example for dolomite the total cation (Ca + Mg) flux (table 1) is $4.2 \times 10^{18}$ moles $my^{-1}$. Accompanying this must be a total flux of $8.4 \times 10^{18}$ eq of negative charge per million years. Subtracting from this $0.24 \times 10^{18}$ eq $my^{-1}$ ($2 \times 0.12 \times 10^{18}$ moles $my^{-1}$) for divalent $SO_4^{--}$ derived from $H_2SO_4$ weathering, we obtain $8.16 \times 10^{18}$ eq $my^{-1}$. This is equal to the flux of $HCO_3^-$ from carbonic acid weathering.

Total anion fluxes, derived in the above manner, for weathering (all in $10^{18}$ moles $my^{-1}$) are:

| | | |
|---|---|---|
| $F_{HCO_3^-}$ dol = 8.16 | $F_{HCO_3^-}$ calc = 16.14 | $F_{HCO_3^-}$ silc = 11.48 |
| $F_{SO_4^{--}}$ dol = 0.12 | $F_{SO_4^{--}}$ calc = 0.23 | $F_{SO_4^{--}}$ silc = 0.16 |

Note that, by far, most weathering of carbonate and silicate minerals consists of attack by $H_2CO_3$ with the formation of $HCO_3^-$ accompanying the cations. However, for the sake of accuracy, especially when dealing with the cycle of $CO_2$, we have separated carbonic and sulfuric acid weathering in order to obtain $HCO_3^-$ weathering fluxes which are as accurate as possible.

Although carbonic acid used in weathering arises from the oxidation of soil organic matter, the ultimate source of this carbon is the atmosphere; soil organic matter is derived from plants that fix atmospheric $CO_2$ via photosynthesis. The fluxes of atmospheric $CO_2$ accompanying the formation of $HCO_3^-$ by weathering can be calculated on the basis of the above data. Of the $HCO_3^-$ carbon derived from silicate weathering all comes (ultimately) from the atmosphere. Of the $HCO_3^-$ carbon derived from carbonate weathering, part comes from the carbonate minerals themselves, and part from the atmosphere. The carbonate mineral contribution is equivalent to the total amount of cations (Ca + Mg); the remainder is derived from the atmosphere. Thus we have (in $10^{18}$ moles per my)

$$\text{For dolomite weathering: } F_{CO_{2_{atm}}} = 8.16 - 4.20 = 3.96$$

$$\text{For calcite weathering: } F_{CO_{2_{atm}}} = 16.14 - 8.30 = 7.84$$

$$\text{For silicate weathering: } F_{CO_{2_{atm}}} = 11.48$$

*Fluxes due to volcanic-seawater reaction.*—There is no doubt (for example, see Holland, 1978; Edmond and others, 1979; Wolery and Sleep, 1976) that a major process by which Mg is removed from seawater is hydrothermal reaction with basalt located beneath mid-oceanic rises. The seawater circulates to considerable depths, where it is heated and reacts with the primary constituents of basalt (volcanic glass, plagioclase, pyrox-

ene, olivine) to form smectites and, at higher temperatures, amphiboles, chlorite, and other hydrous phases (see also the laboratory results of Bischoff and Dickson, 1975; and Mottl and Holland, 1978). These studies have shown that for each $Mg^{++}$ ion taken up by this process there is a stoichiometrically equivalent release of $Ca^{++}$. (Some of this $Ca^{++}$ is precipitated as $CaSO_4$ at depth, but it must ultimately be liberated to solution since $CaSO_4$ is not a common constituent of hydrothermally altered basalts — see Mottl, Holland, and Carr, 1979). Most of the $Mg^{++}$ uptake does *not* involve replacement by $H^+$ ions, as shown both by the laboratory and the field measurements where total net acidities ($Fe^{++}$, $Mn^{++}$, $H^+$ et cetera) of reacted solutions are much lower than that expected for simple $Mg^{++}$–$H^+$ exchange.

There is also evidence, but not generally recognized, for the removal of $Mg^{++}$ from seawater by reaction with volcanic material *at low temperatures*. Throughout much of the south Pacific Ocean surficial sediments are enriched in smectite which has formed by the seafloor alteration of basaltic volcanic ash (Peterson and Griffin; 1964). Low temperature volcanic ash alteration to smectite involves the uptake of $Mg^{++}$ and concomitant release of $Ca^{++}$, just like high temperature alteration. This is shown by the interstitial water studies of Perry, Gieskes, and Lawrence (1976) and Gieskes and Lawrence (1981) who demonstrate decreasing concentrations of dissolved $Mg^{++}$ and increasing concentrations of dissolved $Ca^{++}$ with depth in deep-sea sediments. Thus, the rate of removal of $Mg^{++}$ from seawater by reaction with basaltic material is even greater than that calculated only for hydrothermal reactions at mid-ocean rises.

In contrast to the well-documented situation of removal via volcanic-seawater reaction, removal of Mg (and accompanying $HCO_3^-$) as sedimentary Mg silicates ("reverse weathering" — see Mackenzie and Garrels, 1966) is more controversial. For example, Russell (1970) in studying deltaic sediments of the Rio Ameca, Mexico, found that there was no evidence of authigenic Mg uptake beyond that associated with simple cation exchange. In addition Berner, Scott, and Thomlinson (1970) found no evidence for Mg removal in anoxic siliceous coastal sediments though in disagreement with the results of Drever (1974) and Mackenzie and others (1981). It is true that Sayles (1981) has recently documented slight decreases of dissolved $Mg^{++}$ with depth in deep-sea sediments not obviously associated with volcanic activity, but it cannot be ascertained whether the $Mg^{++}$ loss is due to "reverse weathering" or to a stoichiometric exchange for $Ca^{++}$. If the latter is true, then, whatever processes are occurring in Sayles' sediments, they result in the same overall effect as volcanic seawater reaction, in other words, the uptake of $Mg^{++}$ and release of $Ca^{++}$.

Because of the reasons given above and the fact that virtually no dolomite is forming from the oceans at present, we will assume in the present paper that $Mg^{++}$ added to the oceans by weathering over the past 100 my has been taken up solely by volcanic-seawater reaction, whether high or low temperature. According to this assumption, the uptake is also accompanied by an equivalent release to the oceans of $Ca^{++}$.

(In future work we plan to take a closer look at possible reverse weathering prior to 100 myBP.)

*$CaCO_3$ precipitation.*—As stated in the introduction, there is little or no evidence for dolomite formation from the present oceans. In addition, most workers agree that there is no evidence for appreciable Ca removal as sedimentary Ca-silicates. (The sedimentary Ca-silicates of table 1 refer to detrital phases such as plagioclase or those that have formed from the calcium inherited from detrital phases.) This means that essentially all the $Ca^{++}$ delivered to the oceans, both by weathering and by volcanic-seawater reaction, is removed by the precipitation of $CaCO_3$. The formation of $CaCO_3$, as biogenic skeletal calcite and aragonite in the present oceans, is very well documented, and removal rates are sufficient to account for all incoming Ca (for example, see Berner and Berner, 1984). Thus, in our carbonate-silicate cycle we will balance all inputs of Ca to the oceans ($18.4 \times 10^{18}$ moles $my^{-1}$) by removal as $CaCO_3$. This is an important process and the major way by which $CO_2$ is returned to the atmosphere. The precipitation reaction is the reverse of that for the weathering of calcite given above; in other words:

$$Ca^{++} + 2HCO_3^- \rightarrow CaCO_3 + CO_2 + H_2O$$

(In actuality, precipitation of a small proportion of the $CaCO_3$, $1.02 \times 10^{18}$ moles $my^{-1}$, accompanies the bacterial reduction of $0.51 \times 10^{18}$ moles $my^{-1}$ of $SO_4^{--}$ to pyrite to balance the weathering on land of pyrite to sulfuric acid. The carbon in this $CaCO_3$ is derived from the oxidation of organic carbon and, thus, is not represented in the above reaction. In other words, 18.4 moles of $CaCO_3$ precipitation are accompanied by $18.4 - 1.02 = 17.38$ moles of $CO_2$ liberation, rather than 18.4 moles as predicted by the reaction.)

*Metamorphic (magmatic) fluxes.*—To complete the carbonate-silicate cycle, $CO_2$ must be returned to the atmosphere by the breakdown of carbonate minerals. This is accomplished at elevated temperatures by metamorphic decarbonation reactions and by melting (magmatism) with the release of $CO_2$ by volcanic activity. (Evidence for $CO_2$ degassing via hot springs in areas of magmatic and metamorphic activity has been well documented, for example, Barnes, Irwin, and White, 1978.) For $CO_2$ in the present-day atmosphere not to change too rapidly, $CO_2$ removal and return rates accompanying weathering and the precipitation of $CaCO_3$ in the oceans must be essentially balanced by metamorphism. The balancing flux is $5.9 \times 10^{18}$ moles per $CO_2$ per my. We divide this flux approximately equally between calcite ($2.9 \times 10^{18}$ moles per my) and dolomite ($3.0 \times 10^{18}$ moles per my). Although calcite is more abundant than dolomite (see fig. 1), dolomite is older and more deeply buried and thus, more susceptible to metamorphism and magmatism; thus we assign it equal importance to calcite. Accompanying metamorphism is the stoichiometric transfer of $1.5 \times 10^{18}$ moles $my^{-1}$ each of Ca and Mg from dolomite to the silicate reservoir and $2.9 \times 10^{18}$ moles $my^{-1}$ from the calcite to the silicate reservoir.

*Results.*—The present day carbonate-silicate cycle, based on the values derived above, is shown in figure 1. (Masses of dolomite and calcite are taken from Garrels, Mackenzie, and Hunt, 1975.) Note that, for the sake of simplification, the reservoirs for sedimentary Ca-silicate, igneous and metamorphic Ca-silicate, sedimentary Mg-silicate, and igneous and metamorphic Mg-silicate have all been combined into one reservoir or box. Also, as stated above, the metamorphic fluxes have been adjusted so that all atmospheric $CO_2$ inputs and outputs are balanced.

Some major points are illustrated by figure 1. Note that inputs and outputs to the ocean and atmosphere exactly balance one another. This is done because any appreciable imbalance would rapidly lead to unreasonably large changes in atmospheric $CO_2$. For example, a 10 percent drop in the rate of addition of $CO_2$ to the atmosphere via oceanic $CaCO_3$ precipitation, (all other fluxes remaining constant) would result in the complete removal of atmospheric $CO_2$ in only 30,000 yrs. Such rapid changes do not occur, and, thus, fluxes must be much more closely in balance. (Nevertheless, very small imbalances do exist which, as will be shown later, can lead to major variations of atmospheric $CO_2$ over millions of years.) By contrast with the atmosphere and oceans, fluxes to and from the dolomite and calcite reservoirs do not balance, and this reflects the gradual transfer of mass between the reservoirs according to the reaction discussed in the introduction:

$$CaMg(CO_3)_2 + CaSiO_3 \rightarrow 2CaCO_3 + MgSiO_3 .$$

This transfer over geologic time should result in changes in several of the fluxes because of changes in the masses of material undergoing reaction. Figure 1, thus, serves to set the stage for further consideration in the next section of the carbonate-silicate geochemical cycle and how it has changed with time.

## THE CARBONATE-SILICATE CYCLE OVER THE PAST 100 MILLION YEARS

The cycle diagram shown in figure 1 can be used to represent the carbonate-silicate cycle over geologic time, if the numbers are suitably corrected. In this section we will examine changes brought about over the past 100 my in both the sizes of the reservoirs and fluxes shown on this diagram. Such changes have been brought about, as will be shown, by fluctuations in the rates of weathering, continental runoff, oceanic $CaCO_3$ precipitation, and metamorphic-volcanic $CO_2$ addition to the atmosphere as well as a continuous decrease in the amount of dolomite over this period. Our procedure is to adopt a set of rate law expressions and a reasonable initial condition for the mid-Cretaceous at 100 my ago. The resulting computer program is then run, and all fluxes and sizes of reservoirs are tracked as a function of time up to the present. Initial conditions are readjusted, and the program re-run until the actual present values of fluxes and reservoir sizes are obtained. Once the model is constrained to fit the present cycle it can be used to calculate atmospheric paleo-temperatures, $CO_2$ values, oceanic paleo-pH values, et cetera as a function of time.

In order to simplify calculation we have slightly reduced the values of the fluxes between rock reservoirs and the oceans shown in figure 1 to eliminate the effects of sulfuric acid weathering. In this way complications due to changes in the rates of pyrite weathering and formation with time (for example, see Garrels and Lerman, 1981) are avoided by implicitly assuming at all times a steady-state subcycle involving $H_2SO_4$. In a forthcoming comprehensive treatment, the sulfur (and organic carbon) cycle will be treated explicitly and integrated with the carbonate-silicate cycle, and at that time the numbers given for fluxes in figure 1 will be used without this slight modification. Thus, what we will be considering here is that portion of the carbonate-silicate cycle that involves only weathering by $CO_2$; the weathering uptake fluxes of $CO_2$ from the atmosphere are the same as in figure 1, but the $Ca^{++}$ and $Mg^{++}$ fluxes to the oceans and $HCO_3^-$ fluxes from carbonate weathering are slightly lower as are the metamorphic and volcanic-seawater fluxes used to balance the cycle. The new fluxes are shown, along with the old fluxes taken from figure 1 for comparison, in table 2.

TABLE 2

Present day fluxes in the carbonate-silicate cycle taken from figure 1 and changed to eliminate weathering by $H_2SO_4$

| | | | $10^{18}$ mol $my^{-1}$ | |
|---|---|---|---|---|
| Process | Flux | Species | Value given in figure 1 | Value excluding flux associated with $H_2SO_4$ weathering |
| Weathering | dolomite → ocean | Ca | 2.10 | 1.98 |
| " | " " | Mg | 2.10 | 1.98 |
| " | " " | $HCO_3$ | 8.16 | 7.92 |
| " | calcite → ocean | Ca | 8.30 | 7.84 |
| " | " " | $HCO_3$ | 16.14 | 15.68 |
| " | silicate → ocean | Ca | 2.80 | 2.72 |
| " | " " | Mg | 3.10 | 3.02 |
| " | " " | $HCO_3$ | 11.48 | 11.48 |
| " | atmosphere → dolomite | $CO_2$ | 3.96 | 3.96 |
| " | atmosphere → calcite | $CO_2$ | 7.84 | 7.84 |
| " | atmosphere → silicate | $CO_2$ | 11.48 | 11.48 |
| Calcite formation in ocean | ocean → calcite | Ca | 18.40 | 17.54 |
| Calcite formation in ocean | " " | $HCO_3$ | 18.40 | 17.54 |
| Calcite formation in ocean | ocean → atmosphere | $CO_2$ | 17.38 | 17.54 |
| Volcanic-seawater reaction | ocean → silicate | Mg | 5.20 | 5.00 |
| Volcanic-seawater reaction | silicate → ocean | Ca | 5.20 | 5.00 |
| Metamorphism | dolomite → atmosphere | $CO_2$ | 3.00 | 2.88 |
| " | calcite → atmosphere | $CO_2$ | 2.90 | 2.86 |
| " | dolomite → silicate | Ca | 1.50 | 1.44 |
| " | " " | Mg | 1.50 | 1.44 |
| " | calcite → silicate | Ca | 2.90 | 2.86 |

In order to calculate changes in $CO_2$ over the past 100 my, one must know, in addition to the data of table 2, how fluxes vary with reservoir size, temperature, seafloor spreading rate, et cetera, and how these flux-controlling parameters have varied with time. Thus, a lengthy discussion of fluxes and their rate dependence is given in the next several sections.

*Rate law expressions for weathering.*—In order to calculate ancient fluxes for continental weathering, we have adopted as a starting point the conventional assumption of first order, or linear, reaction rates (see Lasaga, 1981; Garrels and Lerman, 1981). This means that rates of reaction are directly proportional to the mass of material undergoing reaction. (A better approach would be to let weathering be proportional to outcrop *area*, but because determination of outcrop areas as a function of time in the geologic past is very difficult, we will, as a first order approximation, resort to the much simpler mass-proportionality assumption.) Mathematically:

$$F_{W_D} = k_{W_D} D \tag{23}$$

$$F_{W_C} = k_{W_C} C \tag{24}$$

$$F_{W_S} = k_{W_S} S \tag{25}$$

where: $F_W$ = weathering flux of calcium from each process

$D$ = mass of Ca present as dolomite

$C$ = mass of Ca present as calcite

$S$ = mass of Ca present as silicate minerals

$k_W$ = first order rate constant for weathering

and the subscripts D, C, and S refer to dolomite, calcite, and silicate, respectively. Fluxes of Mg from the weathering of dolomite and silicate minerals are directly related to the Ca fluxes via straightforward stoichiometry — for example, $F_W(Ca)/F_W(Mg)$ for dolomite = 1.0/1.0 and for silicates = 2.8/3.1 — see figure 1.

Over time, weathering fluxes are affected by various factors in addition to the mass of material undergoing weathering. Thus, we have modified the simple first order model by letting rate constants $k_W$ be functions of other variables affecting weathering. This includes: continental surface area, run-off, temperature, and atmospheric $CO_2$ concentration (as it affects temperature). (The effect of continental elevation on *chemical* denudation is relatively unimportant — see Holland, 1978.)

The variation of continental land area as a result of sealevel changes has been estimated, as a function of time, for the past 180 my by Barron and others (1980). Based on the assumption that changes in land area are directly proportional to changes in total rock weathering, we have calculated changes in fluxes to the ocean from continental weathering for

the past 100 my. This is done in terms of a weathering area correction factor (see fig. 2) denoted as $f_A(t)$:

$$f_A(t) = \text{land area}(t)/\text{present land area} \quad (26)$$

By multiplying $k_W$ by $f_A(t)$, one, thereby, may express variations in weathering flux due to variations in total land area undergoing weathering. (By this calculation we implicitly assume no appreciable changes in area of land, such as desert, not contributing weathering fluxes to the sea, or changes in area of land underlain by silicates versus carbonates. Such corrections require detailed considerations of paleogeography which are beyond the scope of the present study.)

Further changes in weathering fluxes over time, beyond those due to changes in continental area, arise from variations in worldwide air surface temperature as it affects both runoff and rates of weathering. First of all, increased temperatures should bring about an enhancement of the overall hydrologic cycle (see Manabe and Stouffer, 1980; Budyko, 1977) leading to greater continental runoff. Holding other factors constant, increased temperatures should, in turn, accompany increases in atmospheric $CO_2$ due to the atmospheric greenhouse effect. Thus, variations in continental runoff can be related ultimately to changes in atmospheric $CO_2$, if it is assumed that temperature changes over long term (million year) time scales are brought about only by $CO_2$ changes. (Although temperature changes can obviously be brought about by other causes, such as changes in solar insolation, in the present study we will focus only on the quanti-

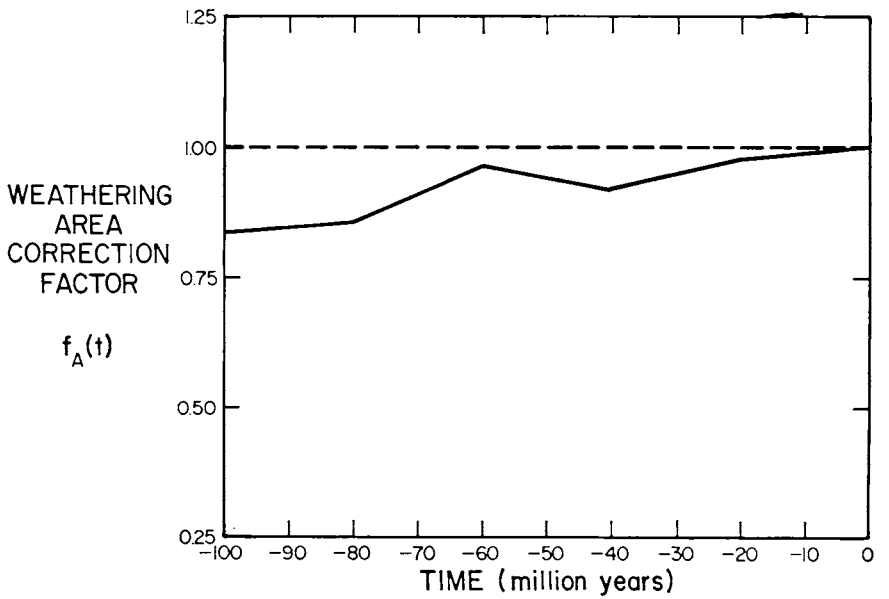


Fig. 2. Weathering area correction factor, $f_A(t)$ as a function of time. Calculated from data of Barron and others (1980). Dashed line represents present day value.

tative significance of $CO_2$ as a temperature control. See later under *Paleoclimatic Implications.*)

We relate runoff to temperature (and atmospheric $CO_2$) in two ways. First of all, the data of Manabe and Stouffer (1980) are used. Manabe and Stouffer present computer-predicted plots of the difference in zonal mean runoff as a function of latitude for the situation of 4 times the present atmospheric $CO_2$ level as compared to the present $CO_2$ level. Averaging over land area and latitude, we obtain an approximate value of $0.54 \times 10^{16}$ liters per yr (0.01 cm per day) for the worldwide increase in runoff accompanying a quadrupling of atmospheric $CO_2$ and corresponding increase in mean annual air surface temperature of 4°C.

Gates (1976) provides data for estimating the decrease in continental runoff accompanying a decrease in air temperature. He presents model-calculated plots of zonally averaged precipitation rate and evaporation rate for the ice-age situation of 18,000 yrs ago, when mean continental temperatures were believed to be about 5°C cooler in the southern (relatively unglaciated) continents of South America, Africa, and Australia and about 10°C cooler in the unglaciated portions of North America, Europe, and Asia. From these plots, along with analogous plots for today, by integrating over latitude we have obtained the approximate change in global mean runoff rate (precipitation minus evaporation) for an average continental temperature decrease of 7°C. It is $1.0 \times 10^{16}$ liters per yr. Combining this result with that derived above from the data of Manabe and Stouffer (1980) we obtain an approximate linear relation between runoff and temperature:

$$R(T)/R(T_0) = 1 + 0.038(T - T_0) \tag{27}$$

where: $R(T)$ = total worldwide continental runoff in liters per yr
$R(T_0)$ = present total worldwide continental runoff ($3.74 \times 10^{16}$ liters $yr^{-1}$)
$T$ = worldwide mean annual surface air temperature (°C)
$T_0$ = present worldwide mean annual surface air temperature.

To correct weathering rate, as embodied in the rate constant $k_W$, it is necessary not only to correct for the effect of temperature on runoff but also for the effect of temperature on rates of mineral dissolution. In other words, we may introduce a temperature correction factor $f_B(T)$ which is given as:

$$f_B(T) = k_W(T)/k_W(T_0) = [c(T)/c(T_0)]\,[R(T)/R(T_0)] \tag{28}$$

where: $c$ = concentration in river water of an element resulting from weathering
$R$ = runoff

The effect of temperature on the weathering rate of carbonate minerals (that is, calcite and dolomite) can be estimated from the data of Harmon and others (1975). Harmon and others, through a study of ground waters across North America, have shown that a highly correlated ($r = 0.966$) simple linear relation exists between the concentration of

$HCO_3^-$ in groundwater resulting from carbonate weathering and temperature of the groundwater. Since groundwater temperature can be used as a good measure of mean annual air temperature (Harmon and others, 1975), their expression can be used to relate $HCO_3^-$ in river water, resulting from carbonate weathering, to air temperature. To obtain the appropriate relation we simply assume that carbonate-derived ground water is diluted to that level of $HCO_3^-$, found in world average river water, which results from carbonate weathering. In other words, we assume that the temperature coefficient of the $HCO_3^-$ concentration in world average river water which is derived from carbonate weathering is the same as that found by Harmon and others for carbonate-derived ground waters. Recasting their data in terms of relative concentrations we obtain:

$$C_{HCO_3}(T)/C_{HCO_3}(T_o) = 1 + 0.049(T-T_o) \tag{29}$$

Substituting the value $C_{HCO_3}(T_o) = 0.650$mM, (based on the values for the total flux of $HCO_3^-$ from calcite plus dolomite weathering given in table 2 and the runoff value of $3.74 \times 10^{16}$ liters per yr) eq (29) can be rewritten as:

$$C_{HCO_3} = 0.650 + 0.0320(T-T_o) \tag{30}$$

Eqs (29) and (30), then, express the concentration of $HCO_3^-$ in world average river water, arising from the weathering of carbonate minerals, in terms of mean annual air temperature.

Combining eqs (27), (28), and (29), we obtain changes in weathering rate constants for dolomite and calcite weathering, expressed as $f_R(T)$, in terms of the mean annual global air surface temperature. This is done, in tabular form, using actual values for $C_{HCO_3}$ and runoff, in table 3. To convert air temperature to atmospheric $CO_2$ content the theoretical results of Manabe and Stouffer (1980) are used, based on their global climate model which combines atmospheric circulation modeling and continental and oceanic heat and water balancing with atmospheric greenhouse effects due to changes in $H_2O$ vapor and clouds, as well as $CO_2$. Their results for 2 times and 4 times the present $CO_2$ level are combined with the observations of W. Berner, Oeschger, and Stouffer (1980) of $CO_2$-depleted, entrapped air bubbles in buried Pleistocene glacial ice, to obtain the empirical relation:

$$\frac{A_{CO_2}(t)}{A_{CO_2}(o)} = \exp[0.347(T-T_o)] \tag{31}$$

where: $A_{CO_2}(t)$ = mass of atmospheric $CO_2$ at time t
$A_{CO_2}(o)$ = mass of atmospheric $CO_2$ today ($0.055 \times 10^{18}$ moles)
T = mean annual global air surface temperature in degrees Celsius at time t

This relation is in essential agreement, within acceptable error for the purposes of the present study, with the calculated values of Augustsson and Ramanathan (1977) (CTA version) and Walker, Hays, and Kasting (1981) for $CO_2$ levels higher than at present. Values of $CO_2$ corresponding to various temperatures are also listed in table 3.

Although no data exist on the effect of temperature on $HCO_3^-$ in ground waters from silicate weathering, it will be assumed here that the temperature (and $CO_2$) effect on silicate weathering is identical to that on carbonate weathering. In other words, the values of $f_B(T)$ given in table 3 also refer to silicate weathering. This is reasonable in that Drake and Wigley (1975) have shown that the empirical relation between carbonate weathering and temperature found by Harmon and others (1975) is best explained in terms of an increase in rates of production of $CO_2$ in soil with increase in temperature. In other words, changes in rates of weathering of carbonate minerals (and silicate minerals by analogy) with temperature are a direct result of changes in metabolic rates of organic matter oxidation (to $CO_2$) with temperature. Both carbonate and silicate minerals are attacked by biogenically-derived soil $CO_2$ resulting in the liberation of $HCO_3^-$ and cations to solution. (See earlier section on weathering fluxes.)

Eqs (28) and (31) can be combined to obtain an analytic relation between weathering flux and atmospheric $CO_2$ concentration. If we define $f_B(CO_2)$ as the correction to the present day weathering flux, due to a different $CO_2$ level in the atmosphere, then:

$$f_B(CO_2) = 1.0 + 0.252 \ln\left[\frac{A_{CO_2}}{0.055}\right] + 0.0156\left\{\ln\left[\frac{A_{CO_2}}{0.055}\right]\right\}^2 \qquad (32)$$

where $A_{CO_2}$ is the new atmosphere $CO_2$ content, and 0.055 is the current $CO_2$ content of the atmosphere (both in units of $10^{18}$ moles) (see fig. 1). The function $f_B(CO_2)$ is plotted in figure 3. This relation shows that the

TABLE 3

Continental runoff R(T), concentration of $HCO_3^-$ in world average river water as a result of calcite-plus-dolomite weathering c(T), and the value of the temperature correction factor $f_B(T) = [cT)/c(T_o)]\ [R(T)/R(T_o)]$ a function of mean annual global air surface temperature T. (Subscript (o) refers to present temperature). Values of atmospheric carbon dioxide mass corresponding to each temperature also shown

| T(°C) | $A_{CO_2}$($10^{18}$moles) | R(T)($10^{16}$liter $yr^{-1}$) | c(T)(mM) | $f_B(T)$ |
|---|---|---|---|---|
| 6 | | 2.45 | 0.362 | 0.36 |
| 8 | | 2.74 | 0.426 | 0.48 |
| 10 | (0.010) | 3.03 | 0.490 | 0.61 |
| 11 | | 3.17 | 0.522 | 0.68 |
| 12 | (0.019) | 3.31 | 0.554 | 0.75 |
| 13 | | 3.45 | 0.586 | 0.83 |
| 14 | 0.039 | 3.60 | 0.618 | 0.92 |
| 15* | 0.055* | 3.74* | 0.650* | 1.00 |
| 16 | 0.078 | 3.88 | 0.682 | 1.09 |
| 17 | 0.110 | 4.03 | 0.714 | 1.18 |
| 18 | 0.156 | 4.17 | 0.746 | 1.28 |
| 19 | 0.220 | 4.31 | 0.778 | 1.38 |
| 20 | 0.312 | 4.46 | 0.810 | 1.49 |
| 22 | 0.624 | 4.74 | 0.874 | 1.70 |
| 24 | 1.25 | 5.03 | 0.938 | 1.94 |
| 26 | 2.50 | 5.31 | 1.002 | 2.19 |

* — present day values; $CO_2$ equivalent to 300 ppm by volume.

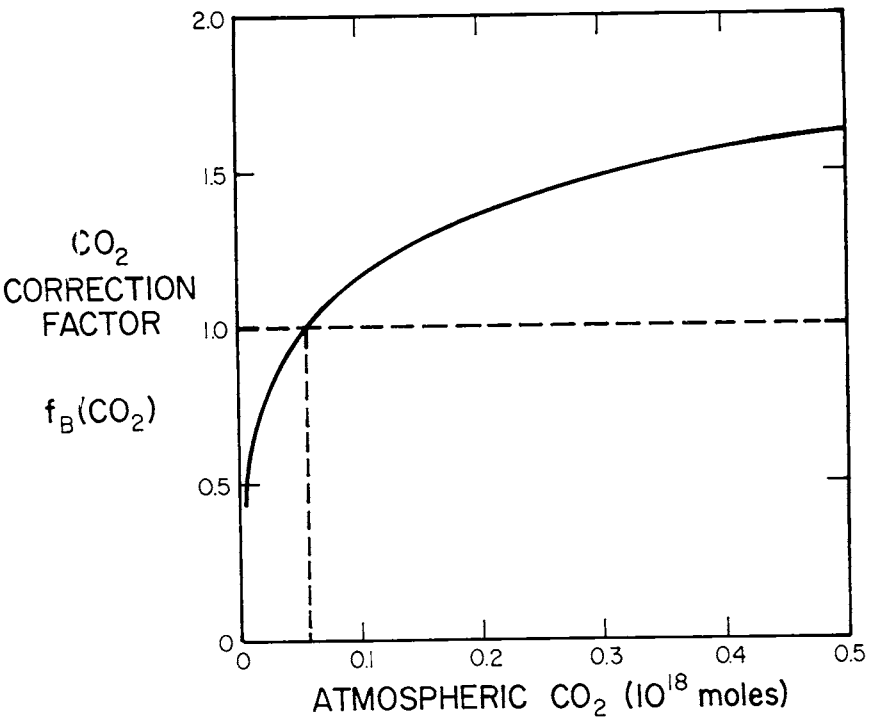


Fig. 3. Carbon dioxide correction factor, $f_B(CO_2)$ as a function of carbon dioxide content in the atmosphere. For derivation of values, see table 3 and eq (32). Dashed lines represent present day values.

rate of uptake of $CO_2$ by weathering is a function, albeit non-linear and indirect, of the level of atmospheric $CO_2$. Thus, a natural negative feedback mechanism against $CO_2$ increases in the atmosphere is provided by weathering. Such a feedback is important in controlling climate and atmospheric $CO_2$ levels as already pointed out by Walker, Hays, and Kasting (1981). However, our feedback, as in Walker's model, is due to changes in temperature and not to any direct effect of *atmospheric* $CO_2$ on weathering rates. Thus, our functional dependence of weathering is not linear with atmospheric $CO_2$ as assumed by Budyko and Ronov (1979) in their $CO_2$ model; instead, increased $CO_2$ causes increased temperatures which in turn cause increased weathering fluxes. We feel that our approach is more realistic than that of Budyko and Ronov, because our $CO_2$ feedback takes into account the importance of (temperature dependent) biological processes as they affect weathering rates. There is no doubt that weathering is dominated by such processes.

By way of summary, one can modify eqs (23), (24), and (25) to take account of changes in land area, expressed as $f_A(t)$, and atmospheric carbon dioxide (temperature) expressed as $f_B(CO_2)$, with time:

$$F_{W_D} = k_{W_D}(o) f_A(t) f_B(CO_2) D \tag{33}$$

$$F_{W_C} = k_{W_C}(o)f_A(t)f_B(CO_2)C \tag{34}$$

$$F_{W_S} = k_{W_S}(o)f_A(t)f_B(CO_2)S \tag{35}$$

where the symbol (o) represents present day $k_W$ values. (Note that the $f_A$ and $f_B$ corrections apply also to $HCO_3^-$ as well as Ca and Mg fluxes.) Since the atmospheric $CO_2$ is also a function of time, we can restate these equations as:

$$F_{W_D} = k_{W_D}(t)D$$

$$F_{W_C} = k_{W_C}(t)C$$

$$F_{W_S} = k_{W_S}(t)S$$

where: $k_{W_D}(t) = k_{W_D}(o)f_A(t)f_B(CO_2)$

$$k_{W_C}(t) = k_{W_C}(o)f_A(t)f_B(CO_2)$$

$$k_{W_S}(t) = k_{W_S}(o)f_A(t)f_B(CO_2)$$

Values of $k_W(o)$ can be obtained from present weathering fluxes (table 2) and reservoir sizes (fig. 1). They are (excluding $H_2SO_4$ weathering):

$$k_{W_D}(o) = 0.00198 \text{ my}^{-1} \tag{36}$$

$$k_{W_C}(o) = 0.00261 \text{ my}^{-1} \tag{37}$$

$$k_{W_S}(o) \cong 10^{-9} \text{ my}^{-1} \tag{38}$$

Note that $k_{W_S}(o)$ is very small due the very large size of the silicate reservoir. Thus, there is little effect of changes in silicate reservoir size on silicate weathering flux on the time scale of 100 my. As a result, silicate weathering rate can be considered to be essentially independent of changes in silicate reservoir size. (Possible exposure of greater *areas* of silicates, relative to carbonates, over time as a result of selective erosion might bring about reservoir size changes, but as mentioned above this lies beyond the scope of the present study.)

*Rate law expression for volcanic-seawater reaction.*—The reactions of volcanic materials with seawater, whether they occur at high or low temperatures, involve mainly the exchange of seawater $Mg^{++}$ for $Ca^{++}$ in primary silicates. Furthermore, because $Mg^{++}$ is quantitatively removed during reaction with hot basalt (Holland, 1978), a simple assumption can be made that $Mg^{++}$ uptake follows first order kinetics. In other words, the rate expression is:

$$F_{Mg_{V-SW}} = k_{Mg_{V-SW}}M_{Mg} \tag{39}$$

where: $F_{Mg}$ = removal flux for reaction of $Mg^{++}$ with volcanics
$k_{Mg}$ = first order rate constant for $Mg^{++}$ removal
$M_{Mg^{++}}$ = mass of $Mg^{++}$ dissolved in the oceans

and the subscript V-SW refers to volcanic-seawater reaction.

The rate constant $k_{Mg}$ includes effects due both to rates of reaction between volcanic minerals and seawater and the rate of flow of seawater (for high temperature reaction) through mid-oceanic ridges. The latter

process should correlate with rates of seafloor spreading (or more strictly, rates of seafloor area generation), and this is what we assume here. If rates of seawater circulation are linearly correlated with spreading rates (a reasonable first-order assumption), then the value of $k_{Mg}$ can be corrected using the spreading rate correction factor, $f_{SR}$:

$$k_{Mg_{V-SW}}(t) = k_{Mg_{V-SW}}(o) f_{SR}(t) \tag{40}$$

where:

$$f_{SR}(t) = SR(t)/SR(o)$$

and SR represents the spreading rate, (t) refers to time, and (o) refers to the present day.

The values used for $f_{SR}(t)$ depend on which model, for the rate of seafloor spreading as a function of time, is adopted. Estimates range from a doubling of spreading rate at 85 my ago (Pitman, 1978; Davis and Solomon, 1981) to less than a 12 percent increase any time over the past 100 my (Parsons, 1982). In the present study we will examine the effects of employing different models for $f_{SR}(t)$ ranging from constant spreading rate, equal to the present day value, to a maximum doubling of the rate in the geological past. Accordingly we will consider four situations. They are: (1) the data of Pitman (1978) for spreading rates over the past 85 my; (2) a revised and corrected version of the spreading rate curve of Southam and Hay (1977); (3) a linear decrease in spreading rate, over the past 100 my, from 20 percent higher than today to the present value; and (4) a constant spreading rate equal to the present value ($f_{SR}(t) = 1.0$).

Plots of $f_{SR}$ versus time, according to these alternative formulations, are shown in figure 4. The curve labelled "Pitman" is calculated from the spreading rate data tabulated for individual ridges by Pitman (1978). The "Corrected Southam and Hay" curve is based on a subduction-corrected version of the spreading rate-versus-time data of Southam and Hay (1977). Southam and Hay's results are based solely on present day areas of seafloor representing different age spans, without correcting for prior loss of portions of older seafloor by subduction. We have corrected for subduction to obtain original areas of seafloor generation by dividing each of their values by the term $\exp(-t/t_m)$, where t = age of seafloor and $t_m$ = maximum age of seafloor = 180 my. This exponential expression represents a probability function for the loss of seafloor by subduction, and it is in rough agreement with the results of Parsons (1982) who points out that, at present, the area of seafloor of a given age-span decreases linearly with age as a result of prior subduction. (However, using the Southam and Hay data, we calculated that there have been considerable fluctuations in the original spreading rate in the past, whereas Parsons suggests that such fluctuations have been minimal.) To present the Parsons minimal-rate-change viewpoint we also include two curves in figure 4, one for a linear decrease of $f_{SR}(t)$ from 1.20 at 100 myBP to today's value, and the other for constant $f_{SR}(t) = 1.00$.

*Rate law expressions for metamorphism-magmatism.*—Release of $CO_2$ via the decarbonation of calcite and dolomite during metamorphism or

igneous melting can be assumed, like weathering, to follow first order kinetics:

$$F_{M_D} = k_{M_D} D \tag{41}$$

$$F_{M_C} = k_{M_C} C \tag{42}$$

Here the subscript M refers to metamorphism-magmatism. The values of $k_M$ for each mineral should change over geologic time as a function of the intensity of decarbonation. Because most decarbonation should take place as a result of heating due to the subduction of sediments (see Barnes, Irwin, and White, 1978), faster rates of seafloor spreading should involve faster rates of subduction, faster rates of decarbonation, and, thus, faster rates of $CO_2$ outgassing, both along the descending plate margins and, after long term transport, at mid-oceanic rises. (For a discussion of the latter, consult Javoy, Pineau, and Allegre, 1982.) In addition, faster $CO_2$ outgassing from below continental interiors should be correlated with greater worldwide tectonism as indicated by increased spreading rate. As a result of these considerations, here the values of $k_{M_D}$ and $k_{M_C}$ are assumed to be linearly correlated with spreading rates, as was the case for $k_{Mg_{V-SW}}$. Accordingly:

$$k_{M_D}(t) = k_{M_D}(o) f_{SR} \tag{43}$$

$$k_{M_C}(t) = k_{M_C}(o) f_{SR} \tag{44}$$

where $f_{SR}$ represents the spreading rate correction factor shown in figure 4.

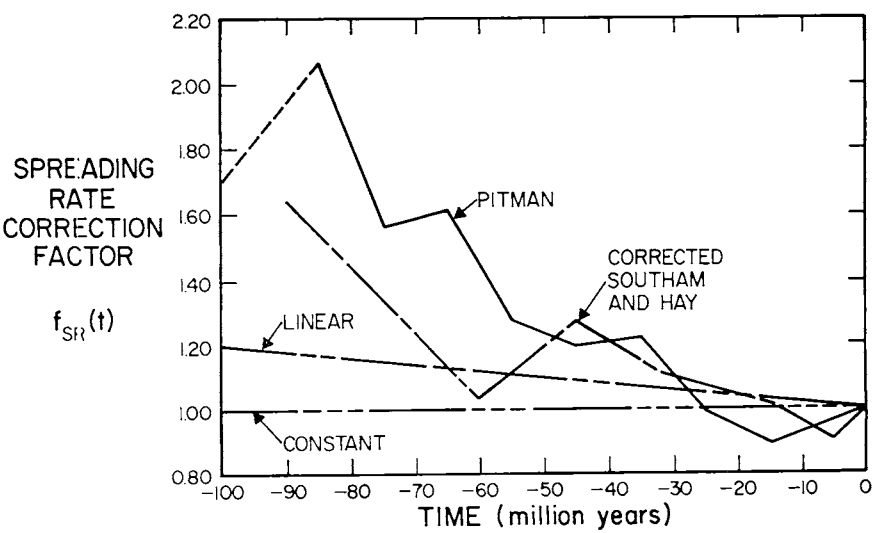


Fig. 4. Four representations of the spreading rate correction factor, $f_{SR}(t)$ as a function of time: (1) calculated from the data of Pitman (1978), (dashed line based on value, assumed here, of $f_{SR}(t) = 1.70$ at 100 my BP). (2) Based on a subduction-corrected version of the curve of Southam and Hay (1977). (3) Assuming a linear decrease in spreading rate from 20 percent higher at 100 my BP; (4) constant spreading rate with time equal to present value.

Present day values of $k_{M_D}(o)$ and $k_{M_C}(o)$, derived from the flux and reservoir size data of table 2 and figure 1, are:

$$k_{M_D} = 0.00144 \text{ my}^{-1}$$

$$k_{M_C} = 0.000953 \text{ my}^{-1}$$

*Rate law expression for calcite precipitation.*—Almost all $CaCO_3$ removal ("precipitation") from the ocean is accomplished by organisms that secrete the carbonate as hard parts. Thus, rates of secretion must be controlled by ecological factors such as the availability of nutrients, and this along with widespread re-dissolution of the carbonate on the seafloor may well lead to rate laws for oceanic carbonate removal that are rather complicated. However, ecological factors cannot dominate to the extent that concentrations of $Ca^{++}$ and $HCO_3^-$ in seawater vary greatly from saturation with calcite (or aragonite); otherwise massive inorganic precipitation or dissolution will take place (as can be readily demonstrated in the laboratory) causing the oceans to return to equilibrium. This suggests that the precipitation rate law for carbonates, on a long-term basis, must take into account that the oceans are maintained reasonably close to saturation with respect to calcite and that the rate law used for the calcite flux should incorporate an appropriate equilibrium expression (that is, there must be no flux at equilibrium). Writing the calcite saturation as:

$$CaCO_3 + CO_{2_{gas}} + H_2O \leftrightarrows Ca^{2+} + 2HCO_3^- \tag{45}$$

yields (using total worldwide masses M, A, rather than concentrations):

$$K_{eq} = \frac{M_{Ca}M^2_{HCO_3}}{A_{CO_2}} \tag{46}$$

Precipitation of calcite is the result of an imbalance in eq (46). Therefore, the calcite flux is written as:

$$F_{calcite} = k_{prep}(M_{Ca}M^2_{HCO_3} - K_{eq}A_{CO_2}) \tag{47}$$

where $k_{prep}$ represents the calcite precipitation rate constant. We must now determine the values of both $k_{prep}$ and $K_{eq}$. First, eq (46) is not exactly equivalent to the equilibrium expressions normally used in computing the composition of a laboratory solution in equilibrium with calcite. The quantities in eq (46) are the total masses of dissolved $Ca^{2+}$ and $HCO_3^-$ in the oceans, $M_{Ca}$ and $M_{HCO_3}$, and the mass of $CO_2$ in the atmosphere, $A_{CO_2}$. Therefore, eq (46) expresses an *effective* equilibrium between "average" concentrations in the oceans and atmosphere. As a result, $K_{eq}$ cannot be best deduced from the $\Delta G°$ of reaction (45). On the other hand, the present day calcite flux shown in table 2 can be used for the value of $F_{calcite}$ in eq (47), thereby obtaining, for known M and A, one equation in the two unknowns. The other equation, needed to derive a value for $k_{prep}$ and $K_{eq}$, is obtained from use of kinetic theory and knowledge of ocean circulation times. The precipitation (or dissolution) of calcite affects the $CO_2$ content of the atmosphere via reaction (45). If we ignore

other processes for the time being, the rate of change of $CO_2$ related to the calcite precipitation/dissolution reaction can be written as:

$$\frac{dA_{CO_2}}{dt} = k_{prep}(M_{Ca}M_{HCO_3}^2 - K_{eq}A_{CO_2}) \tag{48}$$

Recalling that $A_{CO_2}$ is much smaller than $M_{Ca}$ or $M_{HCO_3}$ (see fig. 1), the latter quantities can be assumed constant in studying the changes in $CO_2$ as a result of a perturbation from equilibrium (or steady state). In this case eq (48) can be rewritten:

$$\frac{dA_{CO_2}}{dt} = a - b\,A_{CO_2} \tag{49}$$

where $a = k_{prep}M_{Ca}M_{HCO_3}^2$ and $b = k_{prep}K_{eq}$.
The solution to eq (49) is:

$$A_{CO_2} = \frac{a}{b} - \left(\frac{a}{b} - A^\circ_{CO_2}\right)e^{-bt} \tag{50}$$

Eq (50) readily shows that the response time of the system is given by:

$$\tau = \frac{1}{b} = \frac{1}{k_{prep}K_{eq}} \tag{51}$$

Finally, the response time of the system depends on the time required for $CO_2$ to be dissolved and circulated from the surface to the bottom of the oceans or vice versa. A minimum characteristic time $\tau$ of 500 yrs is used here. (Larger values will be considered later.) Therefore:

$$k_{prep}K_{eq} = \frac{1}{500\ \text{yr}} = 2000\ \text{my}^{-1} \tag{52}$$

Eqs (47) and (52) as well as $F_{calcite} = 17.54 \times 10^{18}$ mol $\text{my}^{-1}$ (table 2) yield the values:

$$K_{eq} = 1721\ (10^{18}\text{moles})^2 \tag{53A}$$

$$k_{prep} = 1.1620\ (10^{18}\text{moles})^{-2}\text{my}^{-1} \tag{53B}$$

which are used in our model.

## OPERATION OF THE MODEL

In this section we outline the computational aspects of our model. First, the initial conditions must be chosen which describe the geochemical cycle 100 my ago, and a major constraint on this choice is that upon integration over time, the final values of the reservoir contents and fluxes, as we arrive at the present, match closely those given in table 2. We will discuss this constraint further below and under *Results.*

Throughout the 100 my period, by far the biggest absolute changes in reservoir sizes occur in the dolomite and calcite reservoirs. Therefore we must assign values to these reservoirs in the initial condition. To arrive at these reservoir values, the present day dolomite weathering and meta-

morphism first order rate constants, $k_w = 0.00198$ my$^{-1}$ and $k_M = 0.00144$ my$^{-1}$ (see table 2) are added to obtain:

$$\frac{dD}{dt} = -0.00342\ D \tag{57}$$

which, upon integration yields:

$$D = D_0 e^{-0.00342\ t} \tag{57A}$$

where D is the reservoir content of dolomite at any time t, and $D_0$ is the present day content of dolomite, that is, $1000 \times 10^{18}$ moles based on figure 1. We can use eq (57) and the value $t = -100$ my to obtain

$$D(-100\ \text{my}) = 1408 \times 10^{18}\ \text{moles}$$

The original D would be slightly different if the rate constants were different in the past. As a first estimate, therefore, the value of $D = 1420 \times 10^{18}$ moles was used for the approximate amount of dolomite 100 my ago. From this value, the corresponding value for the mass of calcite necessary to conserve total carbon at $-100$ my was also calculated (that is, $C = 5000 - 2\ D$, see fig. 1).

To proceed further, a value of $A_{CO_2}$, the $CO_2$ content of the atmosphere 100 my ago, has to be chosen. In the calculations, an arbitrary value $A_{CO_2} = 0.40 \times 10^{18}$ moles was picked. However, as will be shown later, the evolution of the cycle was found to be relatively independent of the initial $CO_2$ value, and the approximate present day (final) value was obtained no matter what starting value was adopted. (This results both from the very small mass of carbon in atmospheric $CO_2$ relative to rocks and the constraint that the present masses of dolomite and calcite be recovered at the end of the calculation.) Because of this a time-consuming self-consistency check on the initial value chosen for $A_{CO_2}$ was not required.

Once an initial $A_{CO_2}$ value is adopted, all weathering rate constants are changed according to the equations given in the previous section to reflect different land area and different $A_{CO_2}$ at $-100$ my. Likewise the volcanic-seawater and metamorphism rate constants are corrected for different spreading rates at $-100$ my. The adjusted rate constants are then used to calculate the calcite precipitation rate required to maintain oceanic steady state 100 my ago. To satisfy the calcite flux, we did not vary the rate constant for precipitation of calcite, $k_{prep}$ or $K_{eq}$, from their present day values as given in eq (53). Rather, the required calcite precipitation flux and the initial value of $A_{CO_2}$ were used to compute the initial values (100 my ago) of $HCO_3^-$ and $Ca^{2+}$ in the oceans, $M_{HCO_3}$ and $M_{Ca}$. To accomplish this, our model ocean ($Ca^{++}$–$Mg^{++}$–$HCO_3^-$), for an initial $M_{Mg}$ equal to that today, requires that:

$$2\ \Delta M_{Ca} = \Delta M_{HCO_3} = 2\ \Delta x$$

where $\Delta M_{Ca}$ and $\Delta M_{HCO_3}$ are the shifts of the initial values (100 my ago) from present day values. Therefore using eq (47)

$$k_{prep}\left[(M^{\circ}_{Ca} + \Delta x)\,(M^{\circ}_{HCO_3} + 2\,\Delta x)^2 - K_{eq}A_{CO_2}\right] = \text{flux} \tag{58}$$

where flux is the calcite precipitation flux required by steady state, and M° refers to the present day values. Eq (58) is solved for Δx to obtain the initial values, $M_{Ca}$ and $M_{HCO_3}$. As mentioned above, the initial value of $M_{Mg}$ is assumed to be the same as that today. (Once the program is run, charge balance is accomplished by $Mg^{++}$ changes as well as by $Ca^{++}$ and $HCO_3^-$ changes.) With these values and the corrected rate constants, $CO_2$ content, and dolomite and calcite masses at −100 my, the initial (quasi) steady state is completely constructed.

Next the system is allowed to evolve through time and values for all variables tracked by numerical (finite-difference) integration of the following non-linear mass balance equations:

$$\frac{dD}{dt} = -(k_{W_D} + k_{M_D})\,D \tag{59A}$$

$$\frac{dC}{dt} = -(k_{W_C} + k_{M_C})\,C + k_{prep}(M_{Ca}M^2_{HCO_3} - K_{eq}A_{CO_2}) \tag{59B}$$

$$\frac{dS_{CaSi}}{dt} = k_{M_C}\,C + k_{M_D}\,D - k_{W_{CaSi}}\,S_{CaSi} - k_{V\text{-}SW}M_{Mg} \tag{59C}$$

$$\frac{dS_{MgSi}}{dt} = k_{M_D}\,D - k_{W_{MgSi}}\,S_{MgSi} + k_{V\text{-}SW}M_{Mg} \tag{59D}$$

$$\frac{dM_{Mg}}{dt} = k_{W_D}\,D + k_{W_{MgSi}}\,S_{MgSi} - k_{V\text{-}SW}M_{Mg} \tag{59E}$$

$$\frac{dM_{Ca}}{dt} = k_{W_D}\,D + k_{W_C}\,C + k_{W_{CaSi}}\,S_{CaSi} + k_{V\text{-}SW}M_{Mg} - k_{prep}(M_{Ca}M^2_{HCO_3} - K_{eq}A_{CO_2}) \tag{59F}$$

$$\frac{dM_{HCO_3}}{dt} = 4\,k_{W_D}\,D + 2\,k_{W_C}\,C + 2\,k_{W_{CaSi}}\,S_{CaSi} + 2\,k_{W_{MgSi}}\,S_{MgSi} - 2\,k_{prep}(M_{Ca}M^2_{HCO_3} - K_{eq}\,A_{CO_2}) \tag{59G}$$

$$\frac{dA_{CO_2}}{dt} = 2\,k_{M_D}\,D - 2\,k_{W_D}\,D - 2\,k_{W_{MgSi}}\,S_{MgSi} - 2\,k_{W_{CaSi}}\,S_{CaSi} + k_{M_C}\,C - k_{W_C}\,C + k_{prep}(M_{Ca}M^2_{HCO_3} - K_{eq}A_{CO_2}) \tag{59H}$$

where D, C, $S_{CaSi}$, $S_{MgSi}$, $M_{Mg}$, $M_{Ca}$, $M_{HCO_3}$, and $A_{CO_2}$ stand for the mass in moles of the dolomite, calcite, Ca-silicate, Mg-silicate, ocean magnesium, ocean calcium, ocean bicarbonate, and atmospheric carbon dioxide reservoirs, respectively. The symbols for the rate constants are the same as defined previously.

A time step of several hundred years was used to integrate the equations through the 100 my interval. The time step size was varied to verify the convergence of the integration. It is important to stress that because

the eqs (59) are *non-linear*, the theoretically possible integration of the equations starting at t = 0 and working back to t = −100 my, is not feasible. This problem stems from the amplification by the non-linear terms of any numerical errors incurred in the backward integration. The non-linearity also limits the use of the general scheme introduced by Lasaga (1980, 1981).

The integrations yield among other things, the atmospheric $CO_2$ content $A_{CO_2}$, and the oceanic $HCO_3^-$ content, $M_{HCO_3}$, as a function of time. Eq (31) is then used to yield the mean global surface temperature as a function of time. (In other words, temperature is assumed to be predictable via the Manabe and Stouffer $CO_2$-climate model.) The reservoir contents, $A_{CO_2}$ and $M_{HCO_3}$, can also be used to obtain the pH of the oceans as a function of time by use of the equation:

$$CO_2(g) + H_2O \rightleftharpoons HCO_3^- + H^+$$

or

$$a_H{}^+ = K_{eq} \frac{A_{CO_2}}{M_{HCO_3}}$$

where the same remarks made about $K_{eq}$ (calcite) in eq (46) are also applicable to the "effective" equilibrium constant, $K_{eq}$ above. Inserting today's values, pH = 8.0 ± 0.2, $A_{CO_2} = 0.055$, and $M_{HCO_3} = 2.8$ (the latter two in $10^{18}$ moles) enables a calculation of $K_{eq} = 10^{-6.29}$. Therefore, at any point in time the pH of surface water can be evaluated from:

$$pH = 6.29 - \log_{10}\left[\frac{A_{CO_2}}{M_{HCO_3}}\right] \tag{60}$$

After an initial trial run, using the values assumed above for the initial masses of dolomite and calcite, the program was re-run using slightly altered dolomite and calcite values that produced final values for D, C, $M_{Ca}$, $M_{HCO_3}$, et cetera that were in closer agreement with actual present-day values. Once this was accomplished, initial values for other parameters were varied to test the sensitivity of the model to such variations. It was found that because of small relative mass, changes in the initial values chosen for $A_{CO_2}$, $M_{Ca}$, and $M_{HCO_3}$ exerted little influence on calculated results beyond the first few million years. In other words, these parameters are dependent on the evolution of the system and not on their starting values. Varying $A_{CO_2}$ up and down by a factor of 5 and using present day values for $M_{Ca}$ and $M_{HCO_3}$ brought about imperceptible changes in time plots after 90 my BP. (Nonetheless, the initial $A_{CO_2}$ was adjusted to minimize those minor errors occurring within the first 10 my.) In addition, varying the value of $k_{prep}$ to reflect changes in the time constant for overturn of the oceans from 500 to 10,000 yrs yielded maximum changes in plots at any given time of less than 2 percent. This means that our model guarantees that the oceans are kinetically close to saturation throughout the past 100 my.

RESULTS AND DISCUSSION

The results for the calculation of atmospheric $CO_2$ and worldwide mean annual air surface temperature, using all the previous expressions and the weathering land area and spreading rate correction curves shown in figures 2 and 4, are shown in figures 5 and 6. Note from figure 5 that calculated $CO_2$ values in the geological past range up to between three times and one-hundred times the present atmospheric value depending on which spreading rate curve is adopted. Regardless of spreading rate formulation, the level of $CO_2$ in the Cretaceous (before 60 my ago) is predicted to have been distinctly higher than exists today and this implies also that there were distinctly higher mean worldwide surface air temperatures at

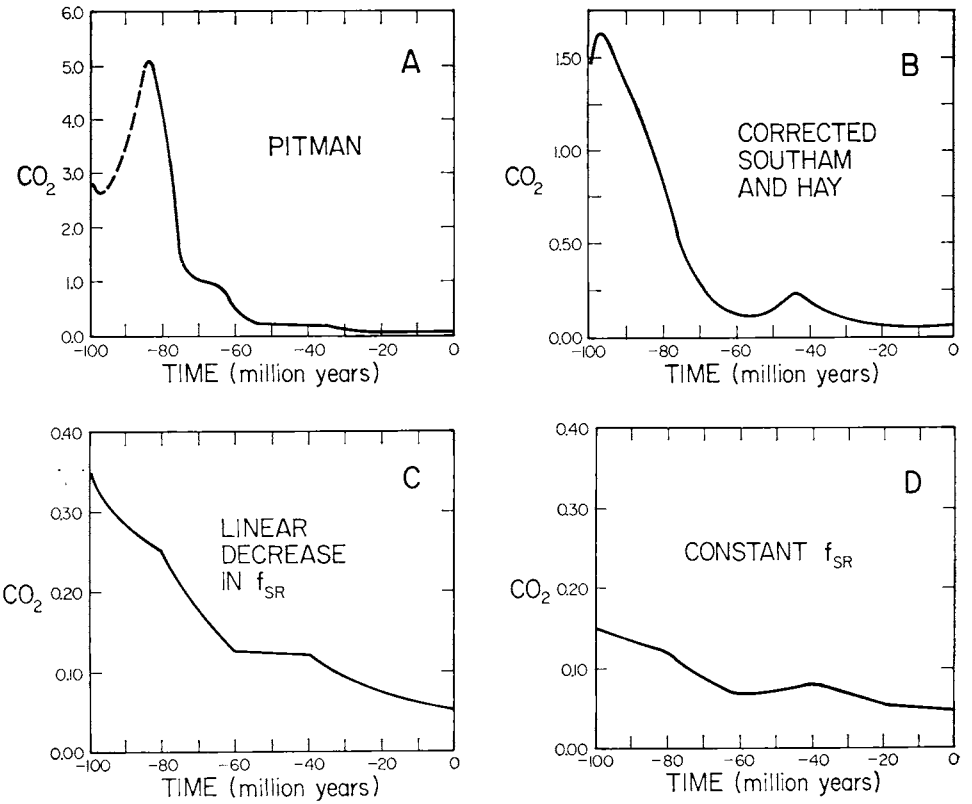


Fig. 5. Computer results for the mass of $CO_2$ (in $10^{18}$ moles) as a function of time for the past 100 my using the land area curve of Barron and others (1980) (see fig. 2) and various spreading rate formulations (see fig. 4 for details on spreading rates):

A. Pitman (1978) spreading rate. (Dashed line based on value, assumed here, of $f_{SR}(t) = 1.70$ at 100 my BP).

B. Southam and Hay (1977) spreading rate corrected for loss by subduction (see text).

C. Linear decrease in spreading rate from 20 percent higher at 100 my BP.

D. Constant spreading rate with time equal to the present value.

NOTE DIFFERENCES IN VERTICAL ($CO_2$) SCALE, BUT WITH THAT FOR C AND D BEING THE SAME.

that time. This is the major finding of the present paper. The temperatures and $CO_2$ levels predicted from the Pitman spreading rate formulation may be too high (see next section on *Paleoclimatic Implications*), and this helps to put some backing behind the contention of Parsons (1982) that changes in spreading rate were considerably lower than those calculated from the Pitman data. However, we are not in a position here to select independently a "best" spreading rate formulation, and this is why all four situations are equally depicted in figures 5 and 6.

One aspect of the corrected Southam and Hay spreading rate formulation, however, commends itself to our attention. It is that, using this approach, we predict (fig. 6B) a secondary temperature maximum centered about 40 my BP which, as will be seen in the next section, is in accord with independent paleoclimatic evidence. Regardless of absolute $CO_2$ values derived, the Southam and Hay curve predicts a pronounced Eocene temperature maximum which is not present or much subdued using the other spreading rate curves.

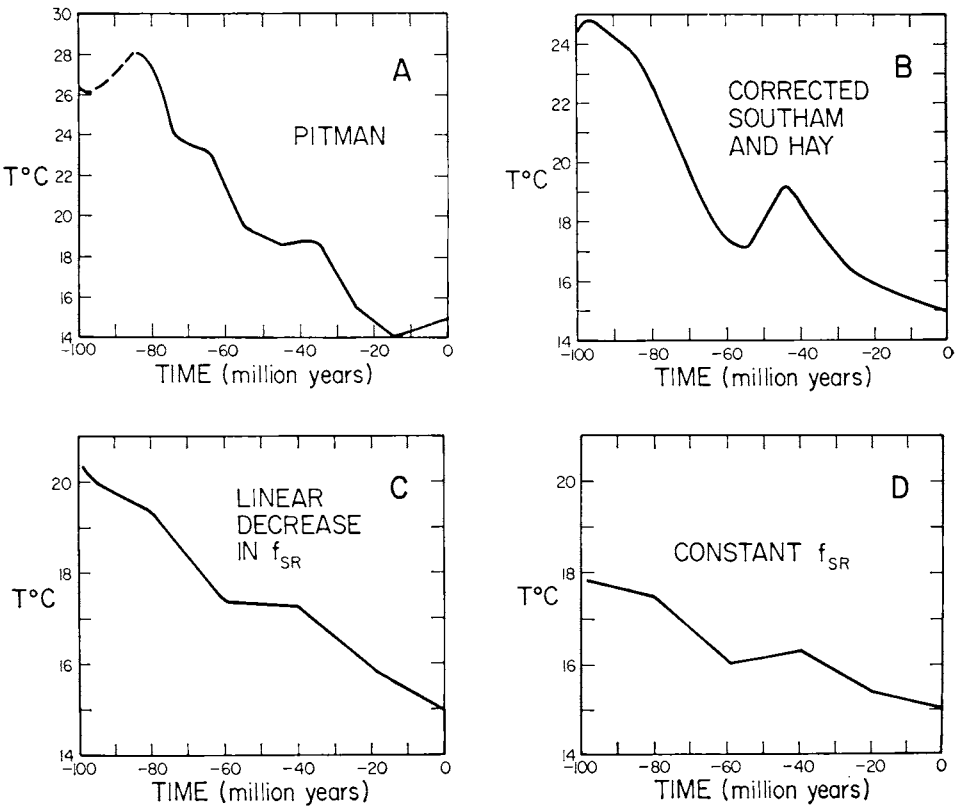


Fig. 6. Computer results for worldwide mean annual air surface temperature as a function of time corresponding to each of the four situations for $CO_2$ depicted in figure 5. NOTE DIFFERENCES IN VERTICAL (TEMPERATURE) SCALE, BUT WITH THAT FOR C AND D BEING THE SAME.

Figures 5 and 6 show how sensitive our results are to changes in spreading rates. What about other factors? In figures 7 and 8 we present some results illustrating sensitivity to changes in land area and to the weathering $CO_2$ correction (feedback) function. Using the corrected Southam and Hay spreading rate formulation, we show in (7A) how $CO_2$ levels and in (8A) how temperatures are altered by holding land area constant with time ($f_A(t) = 1.00$) and in (7B) how $CO_2$ and in (8B) how temperature is affected by using an alternative *linear* functionality for the $CO_2$ weathering feedback factor as employed by Budyko and Ronov

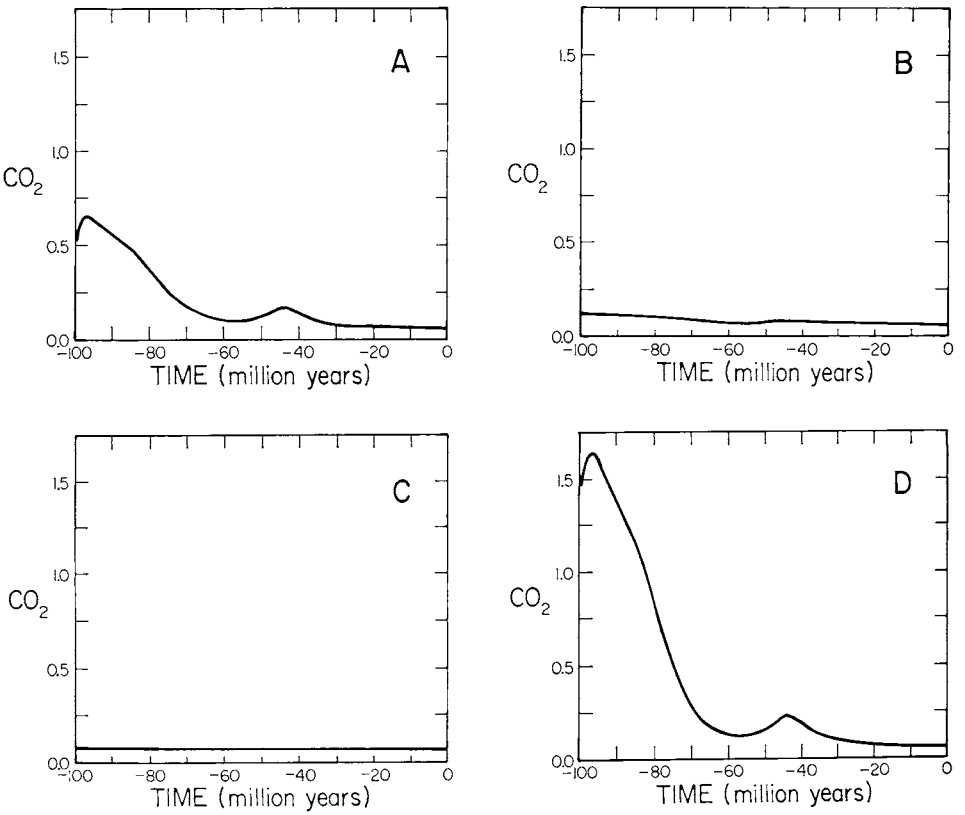


Fig. 7. Effect of varying specific input functions on the mass of atmospheric $CO_2$ (in $10^{18}$ moles) as a function of time.

A. Constant land surface area ($f_A(t) = 1.00$) and spreading rate according to corrected Southam and Hay (1977) curve. Use of eq (32) for $CO_2$ weathering feedback.

B. Changing land surface area according to Barron and others (1980) and spreading rate according to corrected Southam and Hay (1977) curve. Use of linear weathering $CO_2$ feedback function (see text) in place of eq (32).

C. Both constant land surface area ($f_A(t) = 1.00$) and constant spreading rate ($f_{SR}(t) = 1.00$). Use of eq (32) for $CO_2$ weathering feedback.

D. Changing land surface area according to Barron and others (1980) and spreading rate according to corrected Southam and Hay (1977) curve. Use of eq (32) for $CO_2$ weathering feedback (this is a reproduction of fig. 5B).

NOTE FOR ALL CURVES THE VERTICAL ($CO_2$) SCALE HERE IS THE SAME.

(1979). (In place of eq (32) we set $f_B(CO_2) = A_{CO_2}(t)/A_{CO_2}(0)$, where $A_{CO_2}$ refers to the mass of atmospheric $CO_2$, (t) refers to time BP, and (0) to the present.) In addition, in figures 7C and 8C the situation for *both* constant land area ($f_A(t) = 1.00$) and constant spreading rate ($f_{SR}(t) = 1.00$), using the standard $CO_2$ feedback function of eq (32), is presented. Finally, figures 5B and 6B are reproduced in (7D) and (8D) to serve as a reference.

Note in figures 7 and 8 that little $CO_2$ or temperature variation results if both land area and spreading rate are held constant or if a linear $CO_2$ feedback function is used. This, along with the lower Cretaceous values for $CO_2$ and T in figures 7A and 8A compared to 7D and 8D, shows that our predicted results of figures 5 and 6 are sensitive mainly to changes in land area and spreading rates while at the same time being also sensitive to the functional dependence adopted for the weathering feedback function. The almost imperceptible changes depicited in figures 7C and 8C are brought about solely by the monotonic conversion of dolomite to calcite with time and consequent differential weathering. Obviously this

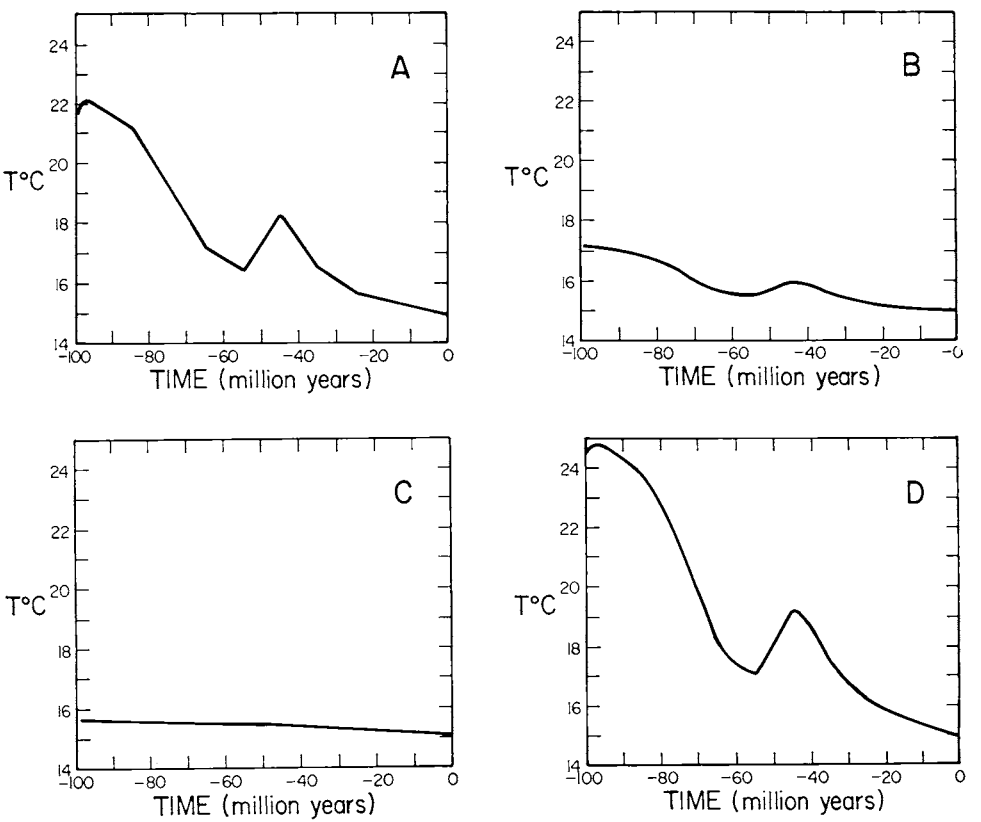


Fig. 8. Effect of varying specific input functions on the mean annual air surface temperature as a function of time. Each curve corresponds to the $CO_2$ situation depicted in figure 7. NOTE THAT VERTICAL (TEMPERATURE) SCALE IS THE SAME FOR ALL PLOTS.

has a far smaller quantitative effect on $CO_2$ than that due to land area and seafloor spreading rate changes.

We feel that the non-linear $CO_2$ weathering feedback function, as embodied in eq (32), is a far more realistic representation of the role of atmospheric $CO_2$ in weathering than use of a simple linear function as portrayed in figures 7B and 8B. The non-linear function, as pointed out earlier during our discussion of weathering, reflects the important observation that weathering rates respond to changes in temperature, as it affects runoff and the microbiological production of *soil* $CO_2$, and that the level of soil $CO_2$ is generally different from and relatively independent of that found in the atmosphere. Thus, we feel that relatively small changes in atmospheric $CO_2$ and temperature, predicted for the use of a linear $CO_2$ weathering feedback function (figs. 7B, 8B), are a consequence of the use of an unrealistic assumption as to the nature of weathering, and, as a result, the larger predicted values of $CO_2$ and temperature shown in figures 5 and 6 are closer to the truth. Regardless of what feedback formu-

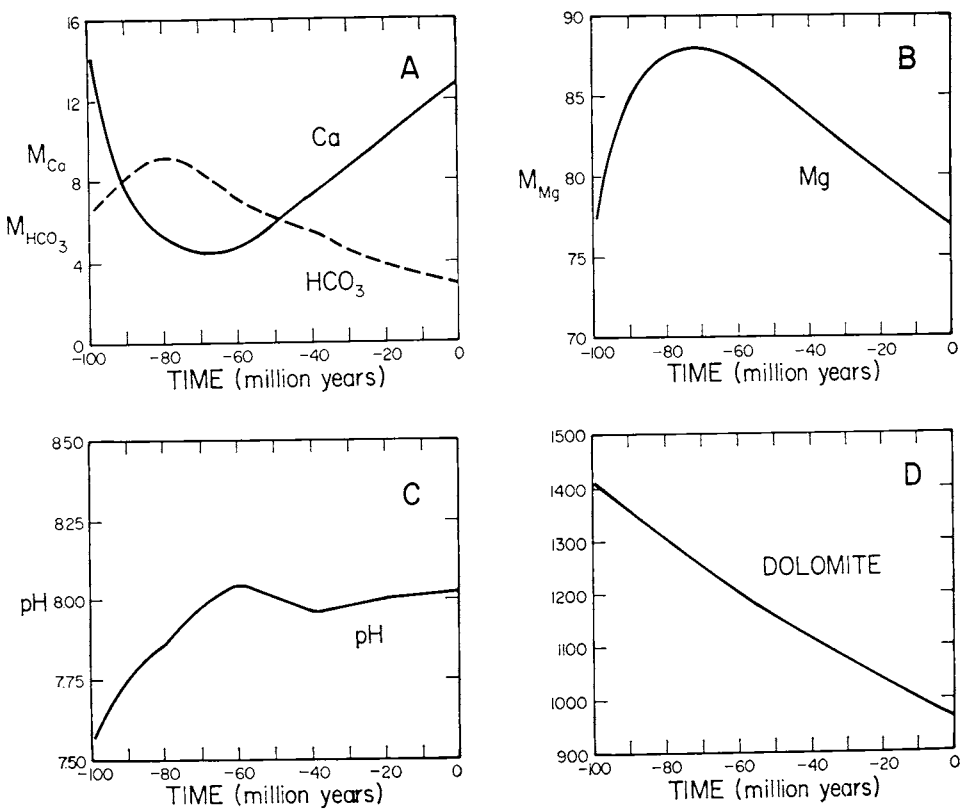


Fig. 9. Computer results for oceanic composition, in terms of $M_{Ca}$, $M_{Mg}$, $M_{HCO_3}$, and pH, and dolomite mass D, as a function of time, for the linearly-decreasing spreading rate formulation (see fig. 4) and land area-versus-time data of Barron and others (1981). Masses in $10^{18}$ moles.

lation is used, it is necessary to have *some* $CO_2$ feedback accompanying weathering. Without any feedback ($f_B(CO_2) = 1$), the values for atmospheric $CO_2$ and temperature grow rapidly with time to impossibly high levels (for example $A_{CO_2}$ attains values in excess of 1000 times the present level).

Resulting changes in the $Ca^{++}$, $Mg^{++}$, and $HCO_3^-$ content and the pH of the oceans, as well as the mass of dolomite, for the linear and corrected Southam and Hay spreading rate formulations, are shown in figures 9 and 10. Note that relatively large changes in $M_{Ca}$ and $M_{HCO_3}$ occur, but that fluctuations, due to changes in spreading rate and land area, are completely damped out for the dolomite reservoir. The smooth exponential-like response of the dolomite reservoir is consistent with its large residence time (>100 my) (for example, see Lasaga, 1981).

The oceanic Ca content decreases and then increases with time in figures 9 and 10. The $HCO_3$ evolution, on the other hand, shows an initial

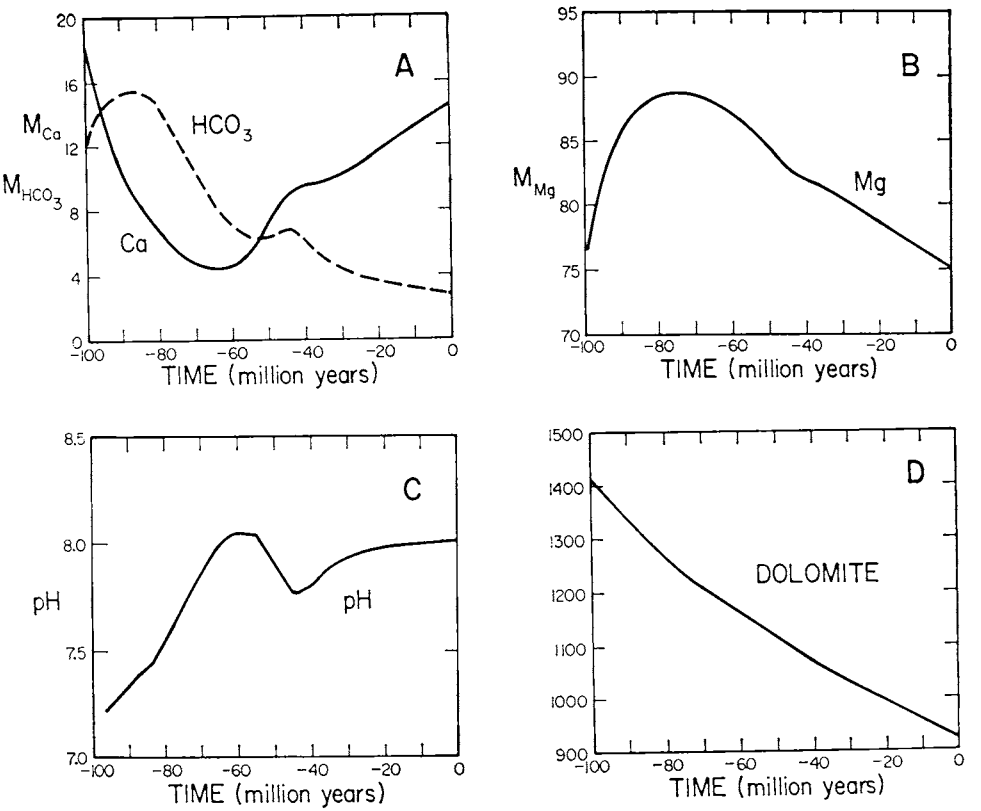


Fig. 10. Computer results for oceanic composition in terms of $M_{Ca}$, $M_{HCO_3}$, $M_{Mg}$, and pH, and dolomite mass D, as a function of time, for the corrected Southam and Hay spreading rate formulation (see fig. 4) and land area-versus-time data of Barron and others (1981). Masses in $10^{18}$ moles.

increase followed by a decrease. Note that the Ca and $HCO_3$ histories, while roughly mirroring each other, are not correlated in a simple manner. The Mg reservoir evolution is likewise the opposite of Ca, namely an initial increase followed by a decrease.

One independent constraint on the fluctuations in the ocean Ca and $HCO_3$ contents has been raised by Holland (1972). Based on the geologic record, the amount of Ca in the oceans must be large enough to precipitate $CaSO_4$ during evaporative concentration without all Ca being removed by earlier $CaCO_3$ precipitation. Consequently, we require that:

$$M_{Ca} > \frac{1}{2} M_{HCO_3}$$

The results shown in figure 9A, for the linear spreading rate assumption satisfy this inequality. However, the results using the corrected Southam and Hay spreading curve (fig. 10A) mildly violate the inequality in the short time span −80 my to −70 my, but this is not too serious.

Average calculated pH values for the entire ocean (figs. 9C and 10C) are reasonably constrained. Initial values at −100 my BP are lower (7.2-7.6) than at present, reflecting the higher atmospheric $P_{CO_2}$ at that time. (This, however, does not mean that the oceans were more undersaturated with respect to $CaCO_3$ in the subsurface than at present, because levels of $Ca^{++}$ and $HCO_3^-$ were correspondingly higher.) From −100 my to about −60 my the pH is predicted to have risen and after that to have fluctuated near the present-day value of 8.0. It is interesting that the calculations do not show excursions to relatively alkaline pH values. Since reverse weathering (authigenic neoformation of silicate minerals at the seafloor) is favored by high pH (greater than 8.5-9.0), this failure to attain elevated pH helps to justify our assumption that, over the past 100 my, reverse weathering has not been an important process for the removal of $Mg^{++}$ from seawater.

A simple method can be used to evaluate semi-quantitatively the effects of changes in various rates on atmospheric $CO_2$. This rests on the fact that, because the $CO_2$ content is so small, it must always be very close to a quasi-steady state:

$$\frac{dA_{CO_2}}{dt} \approx 0 \tag{61}$$

Therefore, using eq (59H) and ignoring the fact that the rate constants are themselves functions of $CO_2$, we can solve for $A_{CO_2}$:

$$A_{CO_2} = \frac{2(k_{M_D} - k_{W_D})D + (k_{M_C} - k_{W_C})C - 2F_{W_{Si}} + k_{prep}M_{Ca}M^2_{HCO_3}}{k_{prep}K_{eq}} \tag{62}$$

Eq (62) can be used to analyze $CO_2$ evolution. One of the basic questions of interest is the role that the dolomite breakdown has in $CO_2$ formation. A major overall reaction occurring in our cycle is the transformation of dolomite to calcite with concomitant changes in the silicate reservoirs:

$$CaMg(CO_3)_2 + CaSiO_3 \rightarrow MgSiO_3 + 2CaCO_3 \tag{63}$$

As a result, the changes in the dolomite and calcite reservoir contents, $\Delta D$ and $\Delta C$ respectively, are related according to eq (63):

$$\Delta C = -2\Delta D \tag{64}$$

Using eq (64) in eq (62), we can determine the shift in the quasi-steady state $CO_2$ content as a result of changes in the mass of dolomite:

$$\Delta A_{CO_2} = \frac{2(k_{M_D} - k_{M_C} + k_{W_C} - k_{W_D})\Delta D}{k_{prep}K_{eq}} \tag{65}$$

The dolomite content is constantly decreasing from the Cretaceous to the present; therefore, $\Delta D < 0$. Substituting present values from table 2 we obtain for $(k_{M_D} - k_{M_C} + k_{W_C} - k_{W_D})$ a positive number. Therefore, from eq (65) the value of $\Delta A_{CO_2}$ should be negative. This was actually found to be the case for the complete computer model, where $CO_2$ was found to decrease with time toward the present. However, this decrease is very small and almost imperceptible on the scale shown in figure 7C.

Another use of eq (65) is in predicting the relative importance of dolomite metamorphic-magmatic decarbonation, as opposed to calcite decarbonation, as it affects atmospheric $CO_2$. The rate constants for weathering, $k_{W_D}$ and $k_{W_C}$, are reasonably well constrained by the available data. By contrast, only the *total* metamorphic flux, given in table 2, is well-constrained. Therefore, it is fruitful to analyze the effect of shifting the metamorphic flux differently between calcite and dolomite from that shown in table 2. An increase in $k_{M_D}$–$k_{M_C}$ should increase the $CO_2$ effect according to eq (65). In table 2 the total metamorphic flux of $CO_2$, 5.74, is split into 2.88 for dolomite and 2.86 for calcite. Instead we will here increase the dolomite metamorphic flux to 4.0 and reduce the calcite flux to 1.74. The cycle is allowed to evolve on the computer with these changes and with *no* changes with time in weathering area or spreading rate. The result for $CO_2$ is shown in figure 11, where it is compared with the result for the fluxes given in table 2. Note that it is clear that the increase in $k_{M_D}$-$k_{M_C}$ has affected the $CO_2$ and temperature histories in accord with eq (65). However, the changes again are not nearly as large as in figure 5. In other words, the dolomite reaction (63), which of itself does not consume or produce any $CO_2$, can lead to a higher $CO_2$ in the Cretaceous, but the change is very small compared to that brought about by spreading rate and land area changes. Analogous calculations for *decreasing* $k_{M_D}$–$k_{M_C}$ give similar results.

The above calculations indicate that the most important influence in the carbonate-silicate geochemical cycle is clearly tectonic history, as it affects spreading rate and land area changes. The tectonic effects are also explained by use of eq (62). Even at constant D and C, increases in spreading rate would yield increases in both $k_{M_D}$ and $k_{M_C}$. Increases in these k's will clearly lead to increases in $A_{CO_2}$ using eq (62). Similarly from (62), decreases in weathering rates arising from decreases in land area would also lead to increases in $A_{CO_2}$. It is important to note that these tectonic changes in $A_{CO_2}$ do not depend on *differences* in the rate constants and

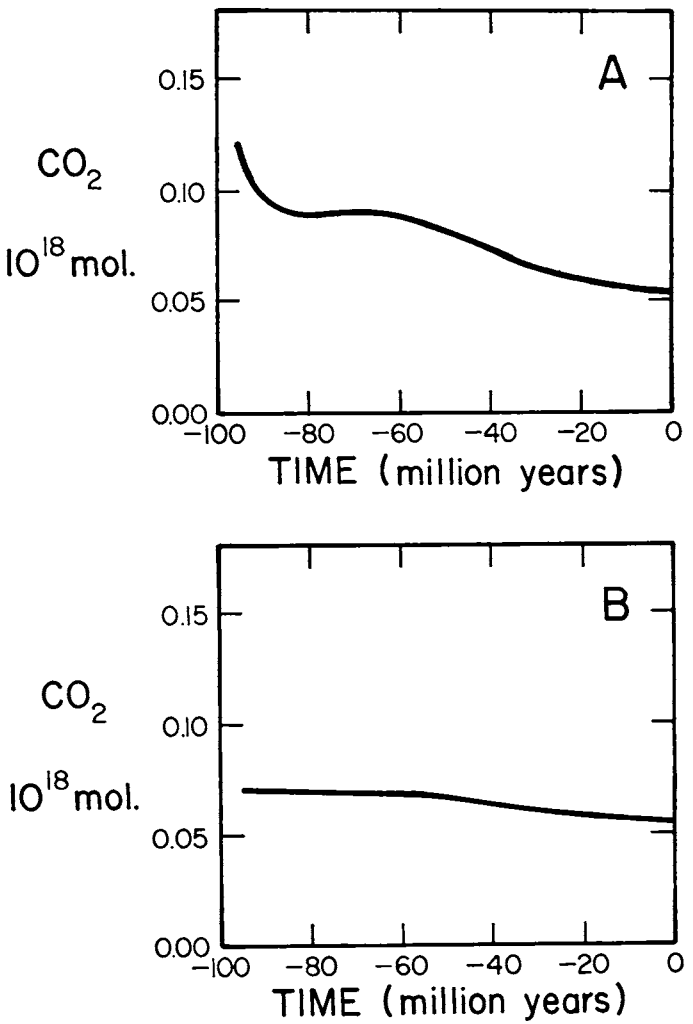


Fig. 11. Atmospheric $CO_2$ for constant seafloor spreading rate ($f_{SR}(t) = 1.00$), constant surface area of land with time ($f_A(t) = 1.00$), and:

A. $F_{M_D} = 4.00 \times 10^{18}$ moles $my^{-1}$ ($k_{M_D} = 0.0020\ my^{-1}$)
$F_{M_C} = 1.74 \times 10^{18}$ moles $my^{-1}$ ($k_{M_C} = 0.00058\ my^{-1}$)

B. $F_{M_D} = 2.88 \times 10^{18}$ moles $my^{-1}$ ($k_{M_D} = 0.0014\ my^{-1}$)
$F_{M_C} = 2.86 \times 10^{18}$ moles $my^{-1}$ ($k_{M_C} = 0.00095\ my^{-1}$)
(see also fig. 7C)

hence are more marked than those stemming from the transformation of dolomite to calcite (eq 65). Finally, it should be stressed that quantitative use of eq (62) can be done only if the variations in $M_{Ca}$ and $M_{HCO_3}$ (which are ignored in eq 65) are properly accounted for, especially since this term is the biggest one in eq (62). However, qualitatively, eq (62) does indeed give an insight into some of the factors playing a role in the $CO_2$ and temperature fluctuations presented in the earlier figures.

Finally the role of organic matter in the $CO_2$ evolution is still not fully settled. Part of the reasoning why organic matter was not included in these calculations is that the isotopic carbon record (Garrels and Lerman, 1981) suggests that the flux of organic matter via weathering to the atmosphere and oceans and the flux of organic matter via burial from the oceans to sediments have not changed significantly in the last 100 my. Preliminary calculations indicate that changing organic carbon burial rates over ranges permitted by the isotopic record has only a moderate effect on atmospheric $CO_2$ and the general trend of decreasing $CO_2$ since the Cretaceous is not appreciably altered; our future work will look at organic matter burial, however, in a quantitative manner and how it relates to atmospheric $CO_2$.

## PALEOCLIMATIC IMPLICATIONS

The carbonate-silicate computer model using reasonable tectonic input data (figs. 5, 6, 9, and 10) predicts that the level of atmospheric carbon dioxide was several-fold greater during the Cretaceous period (60-100 my BP) than it is today. Is this reasonable? We feel that it is. Carbon dioxide in the atmosphere transmits incoming short-wave solar radiation, while absorbing outgoing long-wave earth radiation and returning it to the ground. In this way it acts like a greenhouse trapping the long-wave radiation as heat. (For an up-to-date discussion of the atmospheric "greenhouse effect" see Hecht, 1981; Revelle, 1982.) If there were more $CO_2$ in the Cretaceous atmosphere, there should have been a larger greenhouse effect at that time, and as a result, the climate should have been warmer worldwide. From paleontological, paleobotanical, geochemical, and paleogeographic evidence (for example, see Schwartzbach, 1963; Frakes, 1976; Budyko, 1977; Savin, 1977), this appears to be true. During most of the Cretaceous there was a lack of polar ice caps, high ocean bottom temperatures, wide-spread shallow seas across much of the continents (which should have helped to increase the poleward transport of heat, for example, see Barron, Thompson, and Schneider, 1981), and a spread of low latitude marine and terrestrial organisms to higher latitudes. All these factors indicate a much warmer climate during the Cretaceous than at present. Why couldn't this warming have been due, at least partly, to an increased level of $CO_2$ in the atmosphere? Such a cause for global warming in the past has already been suggested by, for example, Arrhenius (1896), Chamberlin (1898), Callendar (1938), Plass (1956), Budyko and Ronov (1979), and Fischer (1983). Over long (million year) time scales $CO_2$ fluctuations provide a ready explanation for temperature changes which may not be easily explicable in terms of the astronomical-orbital or Milan-

kovitch-type models which have been so successfully applied to shorter term (that is, Pleistocene time scale) oscillations (for example, see Hays, Imbrie, and Shackleford, 1976).

Our predicted evolution of worldwide mean annual surface air-temperature over the past 100 my, using both the linear decrease and corrected Southam and Hay spreading rate curves (fig. 6,B and C), is reproduced in figure 12. Also included in the figure are some estimates of mid-latitude paleotemperatures based on paleobotanical observations and oxygen isotopic studies of marine planktonic calcareous organisms as summarized by Savin (1977). Note that there is reasonably good agreement, especially considering the many problems associated both with our model and the interpretation of paleobotanical and $^{18}O/^{16}O$ data. This gives us some confidence in our model and in our assumption that, over a multi-million year time scale, changes in atmospheric temperature reflect mainly changes in $CO_2$ levels. Regardless of what spreading rate curve is used *we are convinced that the carbon dioxide level of the late Cretaceous atmosphere was higher than it is today, and that this was, at least partly, involved in bringing about higher worldwide air temperatures.* In fact if the data of figure 12 are taken at all seriously, our model, using the corrected Southam and Hay spreading rate curve, also predicts an Eocene temperature maximum, which is in agreement with independent paleobotanical evidence. Obviously our model leaves much ground for improvement especially since eq (31) is an *extrapolation* of the Manabe and Stouffer model to higher $CO_2$ levels not studied by them and to a different paleogeography than exists today. What is sorely needed are new atmospheric climate models based on high $CO_2$ levels and Cretaceous paleogeography (for example, see Barron, Thompson, and Schneider, 1981) as well as, among other things, greater investigations into the phenomenon of metamorphic-magmatic $CO_2$ outgassing and the feedback relation between atmospheric $CO_2$ and rates of weathering. Nevertheless, we feel that at the present stage our results provide a first order attack on the problem. If nothing else, the model indicates that $CO_2$ in the atmosphere *could* easily have changed in the past as a result of geological, as opposed to biological, processes.

Our calculated atmospheric $CO_2$ levels, according to the various spreading rate models (fig. 5), for 70 to 100 my ago, are in rough agreement with that calculated by Budyko and Ronov (1977) from a simple model which assumes that over geologic time $CO_2$ is controlled only by volcanism and the formation of $CaCO_3$ from weathering plus sedimentation. In their model Budyko and Ronov assume that the uptake of $CO_2$ by weathering plus sedimentation of $CaCO_3$ can be described in terms of a simple first order dependence on atmospheric $CO_2$ (with constant coefficient) without consideration of rock type, temperature, oceanic composition, et cetera. We feel that this is oversimplifying the situation and that the rough agreement between their study and ours is fortuitous. Certainly weathering responds to biogenically-produced *soil* $CO_2$ (and organic acids) which in general is not present at levels equivalent to that of the atmosphere.

Regardless of exact $CO_2$ levels and temperatures, our modeling shows the important influence that the carbonate-silicate cycle exerts on atmospheric carbon dioxide. This point has been emphasized by, amongst others, Plass (1956), Budyko (1977), Holland (1978), Mackenzie and Pigott (1981), Garrels (1982), Garrels and Berner (1983), and Fischer (1983). (Plass, Budyko, Mackenzie and Pigott, and Fischer call upon a variety of geological, as opposed to biological, phenomena to explain changes in atmospheric $CO_2$ over the past 500 my.) The reason that the carbonate-

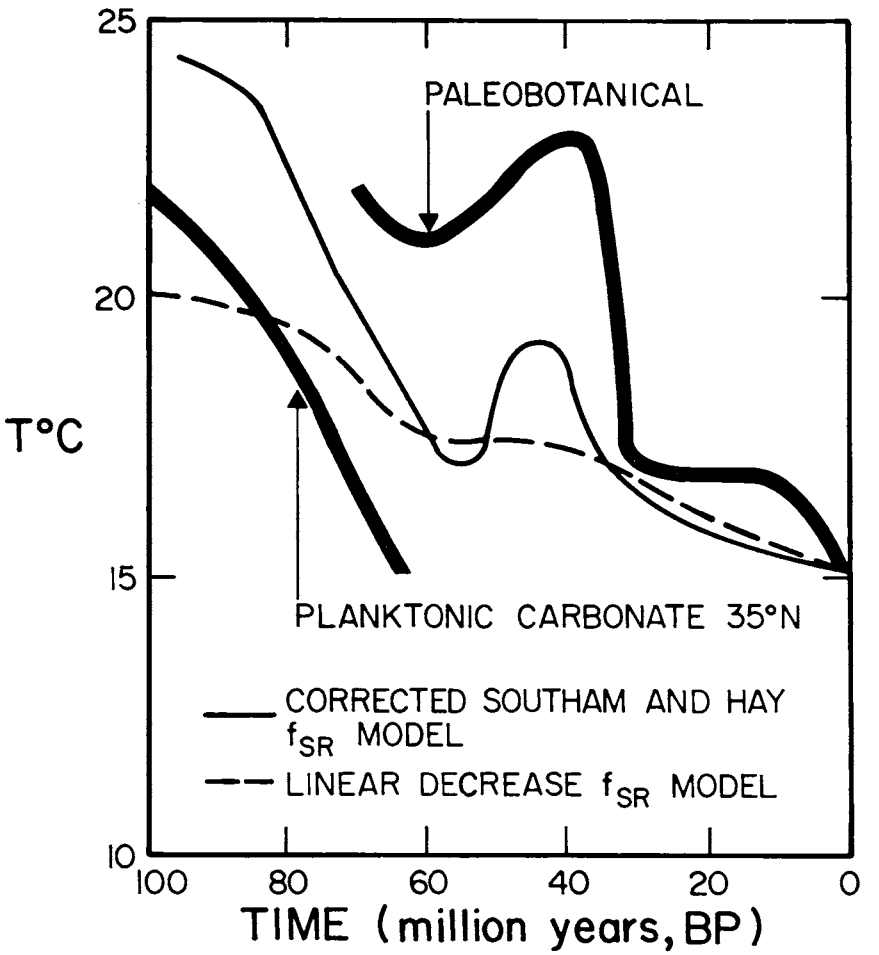


Fig. 12. Plots of worldwide mean annual air surface temperature versus time, based on predictions of the present computer model, compared with some mid-latitude temperatures based on independent evidence. The curve marked "paleobotanical" is based on an average of the results summarized and quantified by Savin (1977, fig. 7) for land plants of Japan, western Europe, and North America, modified to show the steep drop in temperature around 35 my BP found (in a study of leaf margins) by Wolfe and Hopkins (1967). The curve marked "planktonic carbonate 35°N" is an average based on $\delta^{18}O$ studies of planktonic forams and nanno-fossils of Cretaceous sediments of the Shatsky Rise (North Pacific) summarized by Savin (1977, fig. 1C).

silicate cycle is so important is that carbon fluxes between reservoirs are very large compared to the amount of $CO_2$ in the atmosphere. Thus, very slight imbalances in an otherwise steady state cycle can lead to rapid changes (on a geological time scale) in the level of atmospheric $CO_2$.

As pointed out in the *Results Section*, most of the fluctuations we see in atmospheric $CO_2$ over the past 100 my are due to changes in the rates of tectonic processes, as they affect $CO_2$ loss to the atmosphere by metamorphism-magmatism and changes in area of continents exposed to weathering. (Eustatic sealevel rise and drowning of the continents may be due to displaced seawater resulting from increased rates of generation of mid-oceanic ridge basalt via seafloor spreading — see Pitman, 1978.) This conclusion should have applied if we had also considered the weathering and reconstitution of sodium and potassium silicates. Thus, since changes in the rate of sedimentary organic carbon burial over the past 100 my (Garrels and Lerman, 1981) are lower than changes in weathering and metamorphic-magmatic decarbonation rates, the predominant factor affecting atmospheric $CO_2$ and climate over this period, we believe, is worldwide tectonic activity. (Changes in organic carbon burial rate should act in opposition to tectonic processes because calculated burial rates for the Cretaceous are slightly higher than they are today — see Garrels and Lerman, 1981; or Berner and Raiswell, 1983.) This idea of tectonically controlled climate is in agreement with the hypotheses of Hays and Pitman (1973), Fischer and Arthur (1977), Mackenzie and Pigott (1981), and Fischer (1983).

An important additional factor not considered by earlier workers is that brought about by the monotonic decrease in the amount of dolomite available for weathering over the past 100 my. We have shown here that this decrease can also bring about a decrease in atmospheric $CO_2$ level with time, although much smaller than that resulting from tectonic factors. Thus, such subtle effects as changing reservoir size also need to be taken into account when considering geologic controls on atmospheric $CO_2$.

Recently there has been considerable environmental concern over the present-day buildup of atmospheric $CO_2$ due to the burning of fossil fuels. (For a recent summary consult Revelle, 1982.) It is tacitly assumed that changes in atmospheric $CO_2$ are due solely to human activities and that the natural background level is constant with time. Although this may be true for the past 100 yrs, it is most unlikely over longer periods for the reasons given above. Some direct evidence for past changes is provided by recent determinations of the $CO_2$ content of Pleistocene air trapped in glacial ice which shows distinctly lower levels than at present (Berner, Oeschger, and Stauffer, 1980, Broecker, 1982). What is sorely needed are other methods for deducing paleoatmospheric $CO_2$ levels for more ancient times. Only in this way can predictions, as brought out in the present paper, be directly tested.

ACKNOWLEDGMENTS

We acknowledge the partial financial support of NSF Grants OCE 81-09454 and EAR 80-07815 to R. A. Berner, NSF Grant EAR 80-07755

to A. C. Lasaga, and NASA Grant NA6W-339 to R. M. Garrels. We are indebted to the following individuals who provided reviews of the manuscript: L. J. Hickey, F. T. Mackenzie, A. G. Fischer, W. W. Hay, J. R. Southam, E. J. Barron, S. Manabe, J. C. G. Walker, H. D. Holland, and M. L. Bender. We thank E. J. Barron for providing us with data on land area versus time, based on his published research, and B. Parsons for calling attention to his published work on rates of seafloor generation. We have also benefitted from discussions with W. C. Pitman, N. Sleep, T. J. Wolery, E. Sundquist, D. Canfield, B. Saltzman, K. K. Turekian, B. J. Skinner, D. M. Rye, D. H. Zenger, and others too numerous to mention.

## References

Arrhenius, S., 1896, On the influence of carbonic acid in the air upon the temperature of the ground: Philos. Mag., ser. 5, p. 237-275.

Augustsson, T., and Ramanathan, V., 1977, A radiative-convective model study of the $CO_2$ climate problem: Jour. Atmospheric Sci., v. 34, p. 448-451.

Barnes, I., Irwin, W. P., and White, D. E., 1978, Global distribution of carbon dioxide discharges and major zones of seismicity: U.S. Geol. Survey Water Resources Inv., Open-file rept. 78-39, 12 p.

Barron, E. J., Sloan, J. L., II, and Harrison, C. G. A., 1980, Potential significance of land-sea distribution and surface albedo variations as a climatic forcing factor: 180 m.y. to the present: Paleogeography, Paleoclimatology, Paleoecology, v. 30, p. 17-40.

Barron, E. J., Thompson, S. L., and Schneider, S. H., 1981, An ice-free Cretaceous? Results from climate model simulations: Science, v. 212, p. 501-508.

Berner, E. K., and Berner, R. A., 1984, The Natural Water Cycle: Water and Major Elements: New York, Prentice-Hall, in press.

Berner, R. A., 1971, Worldwide sulfur pollution of rivers: Jour. Geophys. Research, v. 76, p. 6597-6600.

———— 1982, Burial of organic carbon and pyrite sulfur in the modern ocean and its geochemical and environmental significance: Am. Jour. Sci., v. 282, p. 451-473.

Berner, R. A., and Raiswell, R., 1983, Burial of organic carbon and pyrite sulfur in sediments over Phanerozoic time: A new theory: Geochim. et Cosmochim. Acta, v. 47, p. 855-862.

Berner, R. A., Scott, M. R., and Thomlinson, C., 1970, Carbonate alkalinity in the pore waters of anoxic marine sediments: Limnology Oceanography, v. 15, p. 544-549.

Berner, W., Oeschger, H., and Stauffer, B., 1980, Information on the $CO_2$ cycle from ice core studies: Radiocarbon, v. 22, p. 227-235.

Bischoff, J. L., and Dickson, F. W., 1975, Seawater-basalt interaction at 200°C and 500 bars: implications for origin of sea-floor heavy metal deposits and regulation of seawater chemistry: Earth Planetary Sci. Letters, v. 25, p. 385-397.

Broecker, W. S., 1983, Ocean chemistry during glacial time: Geochim. et Cosmochim. Acta, v. 46, p. 1689-1705.

Budyko, M. I., 1974, Climate and Life, English edition, Miller, D. H., ed.: New York, Academic Press, 508 p.

———— 1977, Climatic Changes: Am. Geophys. Union (Russian translation), 261 p.

Budyko, M. I., and Ronov, A. B., 1979, Chemical evolution of the atmosphere in the Phanerozoic: Geochemistry Internat., p. 1-9.

Callendar, G. S., 1938, The artificial production of carbon dioxide and its influence on temperature: Royal Meteorol. Soc. Quart. Jour., v. 64, p. 224-237.

Chamberlin, T. C., 1898, The influence of great epochs of limestone formation upon the constitution of the atmosphere: Jour. Geology, v. 6, p. 609-621.

Daly, R. A., 1909, First calcareous fossils and the evolution of the limestones: Geol. Soc. America Bull., v. 20, p. 153-170.

Davis, D. M., and Solomon, S. C., 1981, Variations in the velocities of the major plates since the late Cretaceous: Tectonophysics, v. 74, p. 189-208.

Drake, J. J., and Wigley, T. M. L., 1975, The effect of climate on the chemistry of carbonate ground water: Water Resources Research, v. 11, p. 958-962.

Drever, J. I., 1974, The Magnesium Problem, *in* Goldberg, E. D., ed., The Sea, v. 5: New York, John Wiley & Sons, p. 337-350.

Edmond, J. M., Measures, C., McDuff, R. E., Chan, L. H., Collier, R., Grant, B., Gordon, L. J., and Corliss, J. B., 1979, Ridge crest hydrothermal activity and the balances of the major and minor elements in the ocean: the Galapagos Data: Earth Planetary Sci. Letters, v. 46, p. 1-18.

Fischer, A. G., 1983, The two Phanerozoic subcycles, *in* Berggren, W., and van Couvering, J., eds., Catastrophies in Earth History; The New Uniformitarianism: Princeton, N.J., Princeton Univ. Press, (in press).

Fischer, A. G., and Arthur, M. A., 1977, Secular variations in the pelagic realm: Soc. Econ. Paleontologists Mineralogists Spec. Pub. 25, p. 19-50.

Frakes, L. A., 1976, Climates Throughout Geologic Time: Amsterdam, Elsevier, 310 p.

Garrels, R. M., 1967, Genesis of some ground waters from igneous rocks, *in* Abelson, P. H., ed., Researches in Geochemistry, v. 2: New York, John Wiley & Sons, p. 405-420.

———— 1982, Dialogue between Cyclico and Skeptico: Biogeochem. Newsletter, v. 1, p. 6-8.

Garrels, R. M., and Berner, R. A., 1983, The global carbonate–silicate sedimentary system — some feedback relations, *in* Westbroek, P., and de Jong, E. W., eds., Biomineralization and Biological Metal Accumulation: New York, Reidel, p. 73-87.

Garrels, R. M., and Lerman, A., 1981, Phanerozoic cycles of sedimentary carbon and sulfur: Natl. Acad. Sci. Proc., v. 78, p. 4652-4656.

Garrels, R. M., Lerman, A., and Mackenzie, F. T., 1976, Controls of atmospheric $O_2$ and $CO_2$: past, present and future: Am. Scientist, v. 63, p. 306-315.

Garrels, R. M., and Mackenzie, F. T., 1971, Evolution of Sedimentary Rocks: New York, Norton, 397 p.

Garrels, R. M., Mackenzie, F. T., and Hunt, C., 1975, Chemical Cycles and the Global Environment: Assessing Human Influences: Los Altos, Calif., Kaufmann.

Gates, W. L., 1976, The numerical simulation of ice-age climate with a global general circulation model: Jour. Atmospheric Sci., v. 33, p. 1844-1873.

Gieskes, J. M., and Lawrence, J. R., 1981, Alteration of volcanic matter in deep sea sediments: evidence from the chemical composition of interstitial waters from deep sea drilling cores: Geochim. et Cosmochim. Acta, v. 45, p. 1687-1703.

Harmon, R. S., White, W. B., Drake, J. J., and Hess, J. W., 1975, Regional hydrochemistry of North America carbonate terrains: Water Resources Research, v. 11, p. 963-967.

Hays, J. D., Imbrie, J., and Shackleton, N. J., 1976, Variations in the Earth's orbit: Pacemaker of the Ice Ages: Science, v. 19, p. 1121-1132.

Hays, J. D., and Pitman, W. C., 1973, Lithospheric plate motion, sea level changes, and ecological consequences: Nature, v. 246, p. 18-22.

Hecht, A. D., 1981, The challenge of climate to man: EOS, v. 62, p. 1196-1197.

Holland, H. D., 1972, The geologic history of seawater — an attempt to solve the problem: Geochim. et Cosmochim. Acta, v. 36, p. 637-651.

Holland, H. D., 1978, The Chemistry of the Atmospheres and Oceans: New York, Wiley Intersci., 351 p.

Javoy, M., Pineau, F., and Allegre, C. J., 1982, Carbon geodynamic cycle: Nature, v. 300, p. 171-173.

Lasaga, A. C., 1980, The kinetic treatment of geochemical cycles: Geochim. et Cosmochim. Acta, v. 44, p. 815-828.

———— 1981, Dynamic treatment of geochemical cycles: global kinetics, *in* Lasaga, A. C., and Kirkpatrick, R. J., eds., Kinetics of Geochemical Processes: Reviews in Mineralogy, MSA, v. 8, p. 69-110.

Mackenzie, F. T., and Garrels, R. M., 1966, Chemical mass balance between rivers and oceans: Am. Jour. Sci., v. 264, p. 507-525.

Mackenzie, F. T., and Pigott, J. P., 1981, Tectonic controls of Phanerozoic sedimentary rock cycling: Geology Soc. (London) Jour., v. 138, p. 183-191.

Mackenzie, F. T., Ristvet, B. L., Thorstenson, D. C., Lerman, A., and Leeper, R. H., 1981, Reverse weathering and chemical mass balance in a coastal environment, *in* Martin, J. M., Burton, J. D., and Eisma, D., eds., River Inputs to Ocean Systems: Switzerland, UNEP-UNESCO, p. 152-187.

Manabe, S., and Stouffer, R. J., 1980, Sensitivity of a global climate model to an increase of $CO_2$ concentration in the atmosphere: Jour. Geophys. Research, v. 85, p. 5529-5554.

Meybeck, M., 1979, Concentrations des eaux fluviales in éléments majeurs et approts in solution aux oceans: Rev. Geologie Dynamique et Geographie Physique, v. 21, p. 215-246.

Mottl, M. J., and Holland, H. D., 1978, Chemical exchange during hydrothermal alteration of basalt by seawater I. Experimental results for major and minor components of seawater: Geochim. et Cosmochim. Acta, v. 42, p. 1103-1115.

Mottl, M. J., Holland, H. D., and Carr, R. F., 1979, Chemical exchange during hydrothermal alteration of basalt by seawater II. Experimental results for Fe, Mn, and sulfur species: Geochim. et Cosmochim. Acta, v. 43, p. 869-884.

Parsons, B., 1982, Causes and consequences of the relation between area and age of the ocean floor: Jour. Geophys. Research, v. 87, p. 289-302.

Perry, E. A., Gieskes, J. M., and Lawrence, J. R., 1976, Mg, Ca and $^{18}O/^{16}O$ exchange in the sediment-pore water system, hole 149, DSDP: Geochim. et Cosmochim. Acta, v. 40, p. 413-423.

Peterson, M. N. A., and Griffin, J. J., 1964, Volcanism and clay minerals in the southeastern Pacific: Jour. Marine Research, v. 22, p. 13-21.

Pitman, W. C., 1978, Relationship between eustacy and stratigraphic sequences of passive margins: Geol. Soc. America Bull., v. 89, p. 1289-1403.

Plass, G. N., 1956, The carbon dioxide theory of climatic change: Tellus 8, p. 140-154.

Rubey, W. W., 1951, Geologic history of sea water: Geol. Soc. America Bull., v. 62, p. 1111-1148.

Revelle, R., 1982, Carbon dioxide and world climate: Sci. Am., v. 247, p. 35-43.

Russell, K. L., 1970, Geochemistry and halmyrolysis of clay minerals, Rio Ameca, Mexico: Geochim. et Cosmochim. Acta, v. 34, p. 893-907.

Savin, S., 1977, The history of the earth's surface temperature during the past 100 million years: Ann. Rev. Earth Planetary Sci., v. 5, p. 319-355.

Sayles, F. L., 1981, The composition and diagenesis of interstitial solutions II. Fluxes and diagenesis at the water-sediment interface in the high latitude North and South Atlantic: Geochim. et Cosmochim. Acta, v. 45, p. 1061-1086.

Sayles, F. L., and Mangelsdorf, P. C., 1977, The equilibration of clay minerals with seawater: exchange reactions: Geochim. et Cosmochim. Acta, v. 41, p. 951-960.

Schwarzbach, M., 1963, Climates of the Past: London, D. van Nostrand, 328 p.

Southam, J. R., and Hay, W. W., 1977, Time scales and dynamic models of deep-sea sedimentation: Jour. Geophys. Research, v. 82, p. 3825-3842.

Urey, H. C., 1952, The Planets, Their Origin and Development: New Haven, Yale Univ. Press, 245 p.

Walker, J. C. G., Hays, P. B., and Kasting, J. F., 1981, A negative feedback mechanism for the long-term stabilization of Earth's surface temperature: Jour. Geophys. Research, v. 86, p. 9776-9782.

Wolery, T. J., and Sleep, N. H., 1976, Hydrothermal circulation and geochemical flux at mid-ocean ridges: Jour. Geology, v. 84, p. 249-275.

Wolfe, J. A., and Hopkins, D. M., 1967, Climatic changes recorded by Tertiary land floras in northwestern North America: Pacific Sci. Conf., 11th Tokyo, 1966 Symposium 25 (K. Hatai, ed.), p. 67-76.